Sediment Sampling, Characterization, and Analysis on the Guadalupe River in the Coastal Plain of Texas

University of Houston, Houston, Texas

PIs: K.H. Wang, Professor
Kyle Strom, Associate Professor
Civil and Environmental Engineering

Submitted To: Texas Water Development Board
Research Project: 1348311529
Research Report: Final Report

December, 2015

Sediment Sampling, Characterization, and Analysis on the Guadalupe River in the Coastal Plain of Texas

Kyle Strom[1], Hossein Hosseiny[2], and Keh-Han Wang[3]

Final Report
Sponsor Research Project ID: 1248311361
Research Project Title:"Sediment Sampling, Characterization, and Analysis on the Guadalupe River in the Coastal Plain of Texas"
Sponsored by Texas Water Development Board

December, 2015

Department of Civil and Environmental Engineering
University of Houston
Houston, Texas 77204-4003

[1]Associate Professor, Civil and Environmental Engineering, Virginia Tech, Blacksburg, VA 24061-0105, phone: 540.231.0979, e-mail: strom@vt.edu. Formerly at the University of Houston.
[2]Graduate Research Assistant, Civil and Environmental Engineering, University of Houston.
[3]Professor, Civil and Environmental Engineering, University of Houston.

Abstract

This report presents measured sediment transport data and an effective discharge analysis for four USGS gage stations along the Guadalupe River between Seguin, TX and Victoria, TX. Measurements of channel cross-sectional properties, bed sediment grain-size distribution, suspended sediment concentration, and wash load percentage were made between January 1, 2014 to April 30, 2015 over a range of flow conditions. Bed load transport rates were also measured at the most upstream station (Seguin) over low, moderate, and high discharges to provide the data needed to develop a sediment load rating curve based on measured data for the station. For the remaining three stations, reach property measurements were coupled with sediment transport equations to develop sediment load rating curves. The sediment load rating curves were then used in conjunction with daily and 15-min USGS discharge data to calculate the effective discharge at each of the four stations. Sediment half-load discharges and cross sectional bankfull discharges were also calculated. Field observations and calculations both suggest that bed load is the primary mode of transport at the Seguin, Gonzales, and Cuero sites, and that little bed sediment is moved at discharges less than 2,000 cfs. For flows above 2,000 cfs, the bed load rating curve for the Seguin station was found to be $Q_b = \alpha Q^{\beta}$ with $\alpha = 1\text{E}^{-10}$ and $\beta = 2.8376$. Rating curves for the remaining three sites were developed using an array of standard bed load and total load equations. The β value resulting from these calculations ranged from 1 to 2 with the majority falling between 1.5 and 1.7. Calculated effective discharges were nearly constant across all sites, ranging from 6,200 to 6,900 cfs when using the daily flow data. Variation from station to station increased slightly when using the 15-min data, producing a slight increase in Q_e moving downstream and an overall range of approximately 6,100 to 7,900 cfs. Simple analysis of the yearly peak flow data at the four stations showed that the 1.5 and 2 year floods all increase moving downstream, with the 1.5 year flood increasing from 5,700 cfs to 11,600 cfs from Seguin to Victoria. Half-load discharges were slightly larger than the effective discharges and showed a general increase in value moving downstream from Seguin. Both the effective and half-load discharge were near, but smaller than, the 1.5 year flood at each station. All of the effective, half-load, 1.5 year, and 2 year flows were smaller than the bankfull discharge calculated using the USGS stage-discharge data. This is due to the high banks in this reach of the Guadalupe.

Disclaimer

The contents of this report reflect the views of the author(s), who is (are) responsible for the facts and the accuracy of the data presented herein. The contents do not necessarily reflect the official view or policies of Texas Water Development Board. This report does not constitute a standard, specification, or regulation. This report is not intended for construction, bidding, or permit purposes. Trade or manufacturers names appear herein solely because they are considered essential to the object of this report. The researcher in charge of the project was Dr. Kyle Strom.

Acknowledgements

Kyle Strom and Hossein Hosseiny would like to acknowledge and thank Nolan Raphelt and Mark Wentzel of the TWDB for their cooperation, guidance, and support of the project. We would also like to thank the following graduate and undergraduate students for their help with sample collection and processing: Mohamad Rouhnia, Chengzho Zhang, Jilang Guo, Ali Memariani, Mohammad Hanifzadeh, and Jassim Jaf. Thanks also to Joel Johnson of the Department of Geological Sciences at the University of Texas at Austin and Lindsay Olinde for letting us use their RFID tag antenna and for helping us to get going with the technique.

Contents

List of Figures

List of Tables

1 Introduction

1.1 Project goal and objectives

The goal of this project was to develop a sediment rating curve for one USGS gaging station on the lower section of the Guadalupe River (from Seguin, TX to Victoria, TX), and to calculate the effective discharge at the four USGS gaging stations along the reach. The work was performed in cooperation with the Instream Flow Team of the Texas Water Development Board (TWDB) and focused on obtaining field measurements and calculation of sediment transport at each gaging site over a range of flow conditions. The collected data was then used in developing the annual sediment yield and effective discharge estimates at each station. The specific objectives of the project were to:

1. Collect field data of channel cross sectional geometry, water surface slope, and bed material grain size distribution of the following eight USGS gaging stations.

   (a) 08169792 - Guadalupe River near Seguin, TX

   (b) 08173900 - Guadalupe River near Gonzales, TX

   (c) 08175800 - Guadalupe River near Cuero, TX

   (d) 08176500 - Guadalupe River near Victoria, TX

   (e) 08172000 - San Marcos River at Luling, TX (Tributary)

   (f) 08173000 - Plum Ck near Luling, TX (Tributary)

   (g) 08174600 - Peach Ck near Dilworth, TX (Tributary)

   (h) 08175000 - Sandies Ck near Westhoff, TX (Tributary)

2. Collect field data of sediment transport, including bed and suspended load, at one of the gage stations.

3. Develop sediment rating curves based on the field data and calculations for the four USGS gaging stations on Guadalupe River near Seguin, Gonzales, Cuero, and Victoria Texas.

4. Integrate the sediment rating curves with the annual flow duration curves to produce annual sediment yield histograms and the effective discharge at each of the four gaging stations.

5. Present the work in a written report, scientific journal, and technical conference.

1.2 Overview of approach

Sediment rating curves are site-specific relations that give sediment daily discharge as a function of daily water discharge at a particular river location. Often, the site-specific nature of such relations requires that field measurements of sediment discharge be made over a range of flow

conditions at the location of interest for development of the rating curves. Obtaining this data can be difficult and time intensive. This project focuses on collecting bed load and suspended sediment samples over a range of flow conditions at the Seguin station (gage 08169792). Bed load samples were collected at Seguin with a modified Helley-Smith sampler. Sediment transport rate at the other stations were calculated based on measured cross sectional geometry and sediment grain size distributions. The rating curves at all stations were then used along with the flow frequency histograms developed from USGS discharge data to produce sediment yield histograms. From these histograms the effective discharge for each station was determined (objective 2); the effective discharge is defined as the mean of the discharge increment that transports the largest fraction of the annual sediment load over a period of 10 to 30 years. Sediment yield was also computed for each station by year using the historic daily mean flow data and the developed rating curves (objective 2). This report summarizes the methods, data, and results of the study (objective 3).

1.3 Study sites

The location of the four gaging station sites along the Guadalupe are shown below in figure 1.1, and pictures of the river at each station are given in figures 1.3-1.4. Figure 1.2 shows the location of tributaries and other USGS gage stations in the Guadalupe watershed where data was also collected.

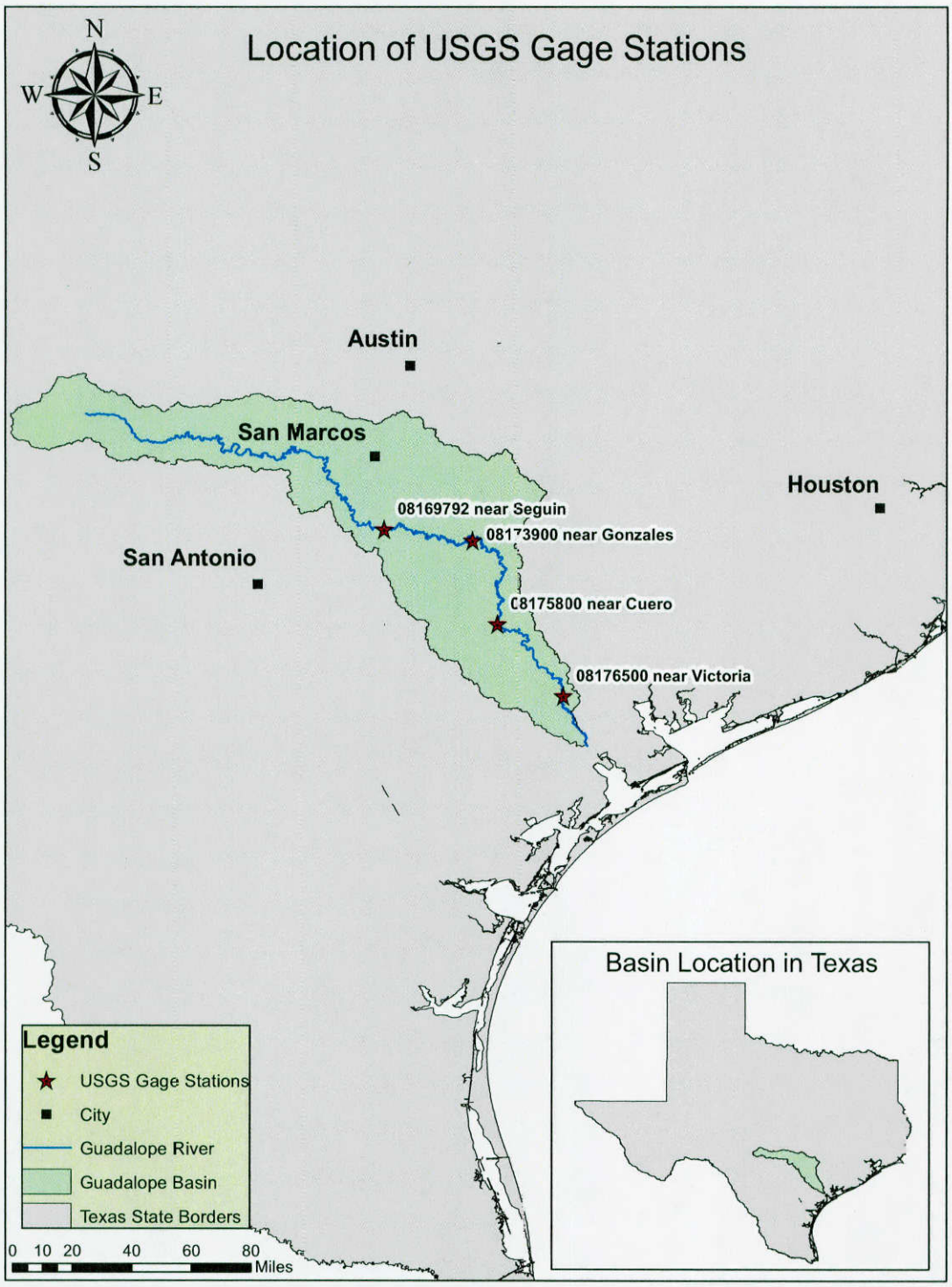

Figure 1.1: A map of Texas showing the Guadalupe watershed and the main gaging stations of the study.

Figure 1.2: A map of the Guadalupe watershed and tributary gaging stations.

Figure 1.3: Pictures of the Guadalupe River from: (A-B) Seguin 08169792 (Google Map image), and (C-D) Gonzales 08173900 (Google Map image). All photos are taken at low flow conditions.

Figure 1.4: Pictures of the Guadalupe River from: (A-B) Cuero 08175800, and (C-D) Victoria 08176500. All photos are taken at low flow conditions.

2 Background

2.1 Effective discharge

Rivers are dynamic entities that self organize in response to imposed tectonic and climatic forces. The concept of a river at "grade" formally put forward by Mackin (1948) is useful for helping to building a framework from which to understand the trajectory of a river with time in response to the imposed boundary conditions. The grade concept simply states that a river reach will modify its slope, through vertical aggradation or degradation and/or lateral change, in such a way as to transport all of the imposed sediment at a given water discharge. This idea was built upon by Lane (1955) who parameterized the concept of a stream at grade as having,

$$QS \propto Q_S d \tag{2.1}$$

where Q is a characteristic dominant volumetric water discharge, S is the channel slope at grade, Q_S is the total bed material sediment load (bed load + suspended load), and d is the characteristic sediment grain size. While the Lane relationship is not dimensionally homogenous, and clearly a simplification, it can be useful for framing the long-term response of a river to boundary conditions changes. For example, if slope increased due to tectonic uplift, then either or both the sediment load and/or size would need to increase at the given water discharge to produce a stream at an equilibrium grade. Or, if sediment load increases but discharge stays constant, the stream would respond by steepening its slope with time (Fig. 2.1). In the transition from one equilibrium state to another, a channel will adjust to the new conditions until the channel comes into a new dynamic equilibrium about the graded state where, on average, there is neither net degradation or aggradation in the channel, i.e., the same volume of sediment leaves the reach as enters it. (Fig. 2.1).

Inherent in the concept of a graded river and the Lane formulation is the notion that the river is responding to some characteristic channel-forming discharge, and that the river itself is alluvial and free to deform its boundaries through erosion of past deposits or deposition of current sediment loads. While a river can be conceptualized as morphologically responding to

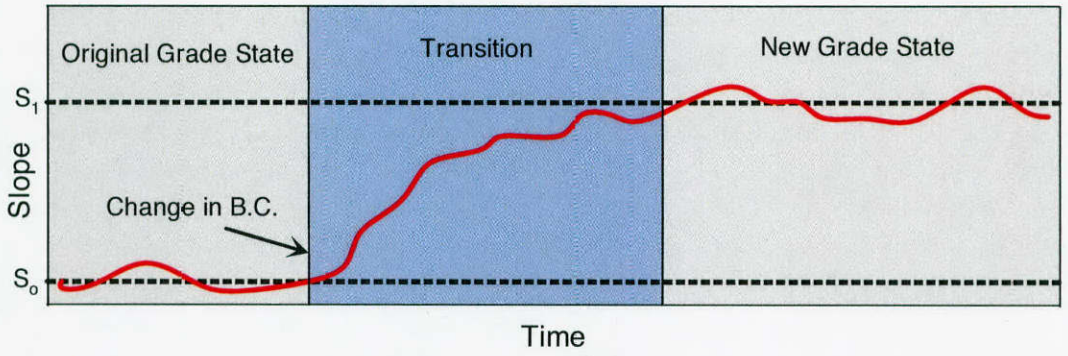

Figure 2.1: Schematic example of a channel adjusting its slope from S_o to S_1 in response to a change in bed material load, Q_b

some characteristic constant discharge, the discharge in natural rivers continually varies over a range of flow conditions, and one is faced with the question of, "what is the dominant channel-forming discharge that the river is morphologically responding to?" This dominant discharge is typically taken to be either the bankfull flow or the effective discharge. The bankfull flow is the discharge that just fills the channel to its banks (identified by a slope break in the stage discharge curve), and the effective discharge is defined as the discharge which moves the greatest percentage of bed material in a river over a given period of time (Wolman and Miller, 1960; Biedenharn et al., 2000). Another way to think about the effective discharge concepts is that it is the discharge that does the most geomorphic work or the discharge that has the most "geomorphic effectiveness" (Wolman and Miller, 1960). Often these two characteristic discharges (bankfull and effective) are fairly close in magnitude and often have return periods on the order of 1 to 2 years (Andrews, 1980; Whiting et al., 1999; Emmett and Wolman, 2001); this, however, is not always the case (e.g., Pickup and Warner, 1976). Another measure of the dominant discharge of a river is the so-called "half-load discharge," $Q_{1/2}$, of Vogel et al. (2003). The half-load discharge is defined as the flow above and below which one half of the total bed material load is transported over a given time period. The half-load discharge is typically associated with a higher magnitude and longer return period flow than the effective discharge (Vogel et al., 2003; Klonsky and Vogel, 2011).

2.2 Calculating effective discharge

Various methods have been used to calculate the conceptualized effective discharge (Wolman and Miller, 1960; Sichingabula, 1999; Crowder and Knapp, 2005; Lenzi et al., 2006; Klonsky and Vogel, 2011). The most often used method is the one proposed by Wolman and Miller (1960), where the probability density function (pdf), or histogram, of the daily mean flow is multiplied by the average daily sediment load associated with each discharge in the distribution to produce a histogram of sediment loads, $S_h = S_h(Q)$, that represents the fraction of load carried by a given discharge, Q, over the time interval of interest,

$$S_h = Q_s f_Q \tag{2.2}$$

Here, $Q_s = Q_s(Q)$ is the daily sediment load (in tons per day) associated with the daily discharge value of Q, and f_Q is the pdf of the daily flow discharges (percent of time that the flow was at a rate of Q). Q_s is the total sediment bed material load and includes contributions from both bed load, Q_b, and suspended load Q_{sbm}. Sediment load histograms of the form of S_h (equation 2.2) can be developed for suspended and bed material load independently and then added together for determination of the effective discharge (Andrews, 1980; Biedenharn et al., 2000), or they can be based solely on suspended or bed load if one transport mode dominates over the other (Wolman and Miller, 1960; Sichingabula, 1999). Often times, the analysis is done using only the suspended load because suspended load is typically the only data easily available (e.g., Klonsky and Vogel, 2011). Typically, in developing the sediment load histogram, S_h, a rating curve that gives the average sediment load as a function of discharge, $Q_s = Q_s(Q)$, is developed from measured data or from sediment transport equations. The sediment load rating curve takes the form of:

$$Q_s = \alpha Q^{\beta} \tag{2.3}$$

where α and β are site-specific coefficients that can be obtained through regression of the Q_s and Q paired data. Once α and β are obtained, the sediment rating equation can be used with the pdf of the daily flow data to produce a histogram that shows the distribution of the percentage of total sediment load as a function of flow rate following equation 2.2 (fig. 2.2). The effective discharge is then selected as the flow rate, Q, associated with the peak in the S_h histogram. Practically, f_Q is constructed as discrete histogram and not a continuous function. When this is the case, the discharge values used in equation 2.2 are those associated with the mid point of each discharge histogram bin (fig. 2.2A), and the effective discharge, Q_e, is the discharge of the mid point of the bin associated with the peak of the histogram.

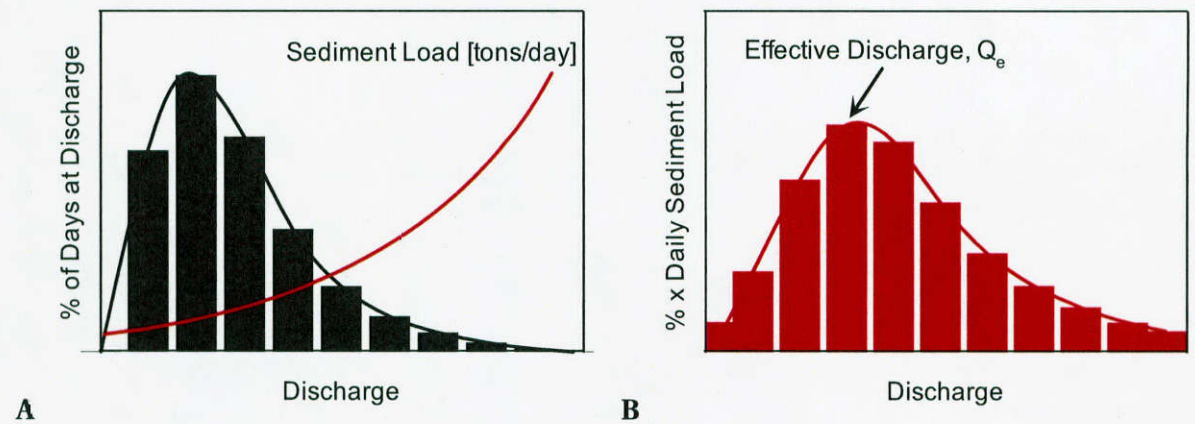

Figure 2.2: Example of a flow duration histogram (A) and a sediment load histogram (B).

2.3 What dictates the location of the peak in the sediment load histogram?

The effective discharge is taken as the discharge associated with the peak in the continuous or discrete sediment load histogram. One can mathematically locate this discharge by taking the derivative of S_h with respect to Q, setting the derivative equal to 0, and then solving for Q. Doing so results in an interesting and useful observation about what impacts the effective discharge calculation for a given site. Theoretically, the effective discharge occurs at:

$$\left.\frac{dS_h}{dQ}\right|_{Q=Q_e} = 0 \tag{2.4}$$

where S_h is the product of f_Q and Q_s at a given discharge, both of which are functions of Q, i.e., $f_Q(Q)$ and $Q_s(Q)$. So, the derivative of S_h can also be expressed as:

$$\frac{dS_h}{dQ} = \frac{d(f_Q Q_s)}{dQ} = f_Q \frac{d(Q_s)}{dQ} + Q_s \frac{d(f_Q)}{dQ} \tag{2.5}$$

Substituting in the rating curve definition for Q_s gives:

$$\frac{dS_h}{dQ} = \alpha\beta Q^{(\beta-1)} f_Q + \alpha Q^{\beta} \frac{d(f_Q)}{dQ} \tag{2.6}$$

Note that setting equation 2.6 equal to zero and dividing by α results in:

$$0 = \beta Q^{(\beta-1)} f_Q + Q^{\beta} \frac{d(f_Q)}{dQ} \tag{2.7}$$

Therefore, if $f_Q = f_Q(Q)$ can be mathematically defined, then one can determine Q_e analytically by solving equation 2.7 for Q. For example, if the pdf of the discharge followed a Gaussian distribution, then:

$$f_Q = \frac{1}{\sigma\sqrt{2\pi}} \exp\left[\frac{-(Q-Q_{avg})^2}{2\sigma^2}\right] \tag{2.8}$$

and,

$$\frac{d(f_Q)}{dQ} = \frac{(Q_{avg}-Q)}{\sigma^3\sqrt{2\pi}} \exp\left[\frac{-(Q-Q_{avg})^2}{2\sigma^2}\right] \tag{2.9}$$

Substituting equations 2.8 and 2.9 into 2.7 would yield a solution for Q, which would be Q_e. It is easy to see in this situation that Q_e is dependent on the characteristics of the flow pdf and on β from the sediment load rating curve:

$$Q_e = Q_e(\beta, \sigma, Q_{avg}) \tag{2.10}$$

In this study, we will develop f_Q using measured data from USGS gaging stations. However, it is still relevant to observe the functionality of Q_e in equation 2.10. Both σ and Q_{avg} are quantities that dependent solely on the measured flow data or analytic flow distribution. This means that for a given flow distribution, the value of Q_e depends solely on the value of β in the sediment load rating curve (equation 2.3); the α value takes no part in setting Q_e.

A logical question following this observation is: what influences the value of β? Using rating curves developed from measured bed load data from rivers in Idaho, Barry et al. (2004) proposed that β is influenced by the degree of armoring in a gravel bed river, with β increasing with the ratio of transport capacity to bed load supply (an index of armoring). β values from their data ranged from 3.5 to 4 for strongly armored beds, down to 1.5 to 2 for beds with little armoring. No further data on the relationship of β to properties of the river have been proposed that we know of. However, it is possible to examine the functionality of β when sediment transport relations and hydraulic resistance equations are used to develop power-law sediment rating curves (equation 2.3). Below we present an outline of this analysis and a summary of the key findings.

Sediment transport equations are typically driven by the average bed shear stress, τ_B. For uniform open channel flows,

$$\tau_B = g\rho RS \tag{2.11}$$

where g is the acceleration of gravity, ρ is the fluid density, R is the channel hydraulic radius and S is the channel bed slope (which for uniform flow is equivalent to the surface slope). For wide channels, R is approximately equal to the channel depth, h, i.e. $\tau_B = g\rho hS$. If τ_B drives transport, then an important functionality in the development of a rating curve for a given reach is:

$$h \propto Q^{b_1} \tag{2.12}$$

Obtaining the functionality of h with Q would allow for τ_B to be set as a function of Q for a wide channel. How exactly h and Q are related is determined by the chosen resistance equation.

Another important functionality that can pop up in the analysis is:

$$U \propto Q^{b_2} \tag{2.13}$$

where U is the cross-sectionally-averaged velocity. However, due to continuity, $b_2 = 1 - b_1$, so determining the functionality of b_1 is sufficient. Again, these functionalities can be used to drive τ_B and hence Q_s to examine the functionality Q_s with Q. We will first look at the value of b_1 when using the Manning-Strickler resistance equation. The procedure will later be generalized to other resistance equations.

For a wide channel, the Manning-Strickler resistance equation is:

$$\frac{U}{u_*} = \alpha_r \left(\frac{h}{z'}\right)^{1/6} \tag{2.14}$$

Assuming a rectangular channel, $Q = Uhw$, where w is the channel width, and using the definition of $u_* = \sqrt{\tau_B/\rho}$, equation 2.14 can be expressed as an explicit function for h:

$$h = \left[\frac{z'^{1/3} Q^2}{\alpha_r^2 g w^2 S}\right]^{3/10} \tag{2.15}$$

or,

$$h \propto Q^{6/10} \tag{2.16}$$

Hence, for this case, $b_1 = 6/10$. Equation 2.15 or the proportionality 2.16 can now be included into sediment transport equations to examine the parameters that influence β in the sediment load rating curves. For example, a general Meyer-Peter and Müller (MPM) type bed load transport equation can be expressed as:

$$q_b^* = \alpha_s \left(\tau^* - \tau_{cr}^*\right)^{\beta_s} \tag{2.17}$$

where the * values are the non-dimensional bed load transport rate and bed shear stress:

$$q_b^* = \frac{Q_b}{w\sqrt{g R_s d^3}} \quad \text{, and} \quad \tau^* = \frac{\tau_B}{(\rho_s - \rho) g d} = \frac{hS}{R_s d} \tag{2.18}$$

τ_{cr}^* is the value of τ^*, i.e., the non-dimensional stress when sediment starts to move. In 2.18 Q_b is the total volumetric bed load transport rate and R_s is the submerged specific gravity, $R_s = (\rho_s - \rho)/\rho$. Using 2.15 and 2.18, equation 2.17 can be written as:

$$Q_b = w\sqrt{g R_s d^3}\,\alpha_s \left(\left[\frac{z'^{1/3}}{\alpha_r^2 g w^2 S}\right]^{3/10} \left[\frac{S^{7/10}}{R_s d}\right] Q^{6/10} - \tau_{cr}^*\right)^{\beta_s} \tag{2.19}$$

If we assuming that the applied stress is significantly greater than the stress needed to cause motion, $\tau^* \gg \tau_{cr}^*$ (a large assumption but reasonable for the proportionality analysis), then it is possible to write 2.19 in the following rating curve form:

$$Q_b \propto Q^{6\beta_s/10} \tag{2.20}$$

Therefore, if $Q_s = Q_b$, then β in the rating curve (equation 2.3) is $\beta = 6\beta_s/10$ or $\beta = b_1\beta_s$, and therefore,

$$Q_b \propto Q^{b_1\beta_s} \tag{2.21}$$

With $b_1 = 0.6$, and the standard Meyer-Peter and Müller (1948) value of $\beta_s = 1.5$, the rating curve power β, becomes 0.9 (that is, $Q \propto Q^{0.9}$). We can perform a similar analysis using the Engelund and Hansen (1967) total load equation,

$$q_s^* = C_f^{-1} 0.05(\tau^*)^{\beta_s} \tag{2.22}$$

instead of the MPM-like bed load equation (2.17). The resulting form of the rating curve using the Engelund and Hansen (1967) total load equation is:

$$Q_s \propto Q^{(2-3b_1+b_1\beta_s)} \tag{2.23}$$

with $\beta_s = 5/2$. Use of the Manning-Strickler resistence equation with $b_1 = 0.6$ therefore results in $Q_s \propto Q^{1.7}$. In 2.22, C_f is the friction coefficient, $C_f^{-1/2} = U/u_*$, and q_s^* is the per unit width dimensionless total load transport rate, $q_s^* = Q_s/(w\sqrt{gR_sd^3})$ where Q_s is the volumetric total load transport rate.

The proportionalities in equations 2.21 and 2.23 reveal something very interesting. That is, the value of β in the rating curve is only dependent on the sediment transport equation selected and the value of b_1. It is not dependent on any of the site specific data such as grain size, channel slope, or the channel width; all of which might be important when making actual estimates of the transport rates. For example, the classic Meyer-Peter and Müller (1948) formula, $\beta_s = 3/2 = 1.5$. Using the classic MPM would therefore produce a $\beta = 1.5b_1$, whereas use of the modified MPM formula of Wong and Parker (2006) would yield $\beta = 1.6b_1$ based on their suggestion that it is more appropriate to let $\beta_s = 1.6$. Likewise, using the Engelund and Hansen (1967) total load equation would result in $\beta = 2 - b_1/2$. Furthermore, when using the Manning-Strickler resistance equation, b_1 is also not a function of any local reach conditions. It is equal to 6/10 regardless of the channel slope, width, or grain size. Taken together, this means that β in the rating curve is only a function of the resistance relation and the sediment transport equation selected to build the rating curve. β is not a function of the local conditions. Coupling this conclusion with the fact that β controls the effective discharge (equation 2.10) means that the exact sediment size, slope, or width of a given reach will not impact the determination of Q_e past guiding one to pick a resistance and transport equation for the analysis.

The above analysis was done specifically for a rectangular channel using the Manning-Strickler resistance equation, a MPM-like bed load transport equation, and the Engelund and Hansen (1967) total load equation. Doing the same analysis with different transport equations and resistance equations, and moving away from a rectangular cross section, all add a bit of nuance to the functionality of β. However, the end results is nearly the same in all cases. Namely, the selection of the resistance and transport equations plays a much larger role in setting β, and hence Q_e, than any specific reach conditions or data. For example, if the Keulegan equation:

$$\frac{U}{u_*} = C_f^{-1/2} = 2.5\ln\left(11\frac{h}{k_s}\right) \tag{2.24}$$

or the Manning equation:

$$U = \frac{C_o}{n}R^{2/3}S^{1/2} \tag{2.25}$$

are used, it can be shown that b_1 in equation 2.12 is weakly dependent on grain size, slope, and channel shape and width. In 2.24, k_s is the roughness length scale that is proportional to the diameter of the d_{50} or d_{84} of the bed sediment; in 2.25, $C_0 = 1.486$ for US customary units and is $C_0 = 1$ for SI; n is the Manning n-value. While these resistance equations do embed some reach-specific functionality into b_1, examining the change in b_1 over a range of reasonable slope and grain sizes leads to only a minor changes (Table 2.1). Over the range of values present in the table, b_1 changes only about 0.05 for the Keulegan equation and up to approximately 0.1 for the Manning equation. Furthermore, a change in b_1 on the order of 0.1 produces a change in β on the order of 0.15 for the MPM type bed load equation (assuming $\beta_s = 1.5$) and 0.1 for the Engelund and Hansen (1967) total load equation. Changes on these order are small relative to the change of ~ 0.7 moving from an MPM-type equation to the Engelund and Hansen (1967) equation. Calculation of β for a several different transport equations shows that β typically falls between 1 and 1.7; values above 2.0 should be considered very steep and outside of the range of typical sediment transport relations where capacity is not limited by sediment supply.

Resistance Eq.		$S = 0.0001$		$S = 0.001$	
		$d_{90} = 3$ [mm] ($n = 0.02$)	$d_{90} = 200$ [mm] ($n = 0.04$)	$d_{90} = 3$ [mm] ($n = 0.02$)	$d_{90} = 200$ [mm] ($n = 0.04$)
Manning-Strickler (eq. 2.14)	$b_1 =$	0.6	0.6	0.6	0.6
Keulegan (eq. 2.24)	$b_1 =$	0.624	0.598	0.62	0.57
Manning (eq. 2.25)	$b_1 =$	0.674	0.706	0.639	0.658

Table 2.1: b_1 values using three different resistance equations for a range of slope and grain sizes.

From the above analysis, it can be concluded that the effective discharge estimates made using calculated sediment transport rates will be set by the pdf of the discharge at a given site and the selection of a given transport equation. The calculation will be relatively insensitive to the grain size, channel slope, channel width, or the exact cross sectional shape used in the analysis.

2.4 Method for constructing the PDF of the flow data

One of the biggest sources of variability in the calculation of the effective discharge comes through the way in which the pdf of the daily flow data, f_Q (also known as the flow frequency and flow duration histogram) is produced (Sichingabula, 1999; Biedenharn et al., 2000; Crowder and Knapp, 2005; Lenzi et al., 2006; Ma et al., 2010; Klonsky and Vogel, 2011). The flow frequency distribution is produced using historical measurements of the discharge over a substantial amount of time (10 or more years if possible); the discharges can be 15-minute, 1-hour, or mean daily data. The discharges are then binned and the percentage in each bin is calculated to create f_Q. Typically, the width of the bins is set manually, and some adjustment to the bin widths may be required to keep the peak in the sediment discharge histogram from occurring in the first bin (Biedenharn et al., 2000). Manual selection of the bin width is based on past experience and some general guidelines such as, starting out by sorting the flow into 25 arithmetically even-spaced bins (Hey, 1997; Biedenharn et al., 2000) and then adjusting bin number/width as

needed. In the end, the exact bin number/width used is the result of trial and error, where the bin numbers are iteratively adjusted until a relatively smooth rising and falling of the sediment histogram has been developed. Developing a representative histogram or pdf of the discharge is key since the shape of the curve, which is determined by bin number/width selection and the historical data, greatly influences the calculation of effective discharge.

3 Methods

3.1 Data needed

The effective discharge and annual sediment yield calculations require (1) historic discharge data for development of the daily flow pdf and (2) sediment load data for the development of sediment rating curves for each gaging station (eq. 2.3). Q_s in equation 2.3 is defined as the total bed material load, which is equal to the bed material load moving in suspension plus the bed material load moving in contact with the bed region, i.e. the bed load. The sediment rating curve for Seguin was developed using physical measurements of the bed load. For the other three stations, measured cross sections and sediment grain size distributions were used along with SamWin to model the hydraulic characteristics and sediment transport rate under a range of flow conditions. Results from the calculations were then used to define the sediment rating curves for those stations.

3.2 Flow conditions and historic flow statistics

Suspended sediment was collected at eight different flow conditions covering a range of high, moderate, and low flow conditions at Seguin. The bed load data were all collected during times of high flows since there was no sediment motion during the low and moderate flows. The relative magnitude of high, moderate, and low flow at each site were based on exceedance values of available historic 15-minute discharge data obtained from the USGS National Water Information System (NWIS) from October 10, 2007 to June 1, 2015. For the study, high, moderate, and low flow were defined as follows: a high flow is a discharge that has historically been exceeded less than 20 percent of the time; moderate flow is a discharge that has historically been exceeded between 20 and 50 percent of the time; and low flow is a discharge that has historically been exceeded between 50 to 90 percent of the time. The specific discharge values at the cuts of 90, 50, and 20 percent of the time exceeded for Seguin can be found in Table 3.1.

		Exceedance Values			Return Periods			Available Data
Station	gage #	$Q_{90\%}$ [cfs]	$Q_{50\%}$ [cfs]	$Q_{20\%}$ [cfs]	$Q_{1.5}$ [cfs]	Q_2 [cfs]	Q_{10} [cfs]	Duration [yrs]
Seguin	8169792	100	400	700	5,723	6,330	-	9
Gonzales	8173900	200	600	1,100	8,408	15,609	108,263	30
Cuero	8175800	200	500	1,100	11,092	15,300	70,561	51
Victoria	8176500	200	500	1,100	11,600	16,500	61,166	80

Table 3.1: Discharge statistics for the percent of time exceeded ($Q_{90\%}$, $Q_{50\%}$, and $Q_{20\%}$) along with the 1.5, 2, and 10 year return period flows calculated by ranking and linear interpolation using available USGS annual peak stream flow data.

3.3 Monitoring and predicting flow conditions

Obtaining enough lead time to drive from Houston, TX to the Seguin gaging station was an important element of the project. The task was complicated by the flashy nature of the river and the number of hydraulic structures and small reservoirs between the nearest upstream gage station and the Seguin site. For example, the discharge can change at a rate of 200 (cfs/hr) for lower high flows, and up 700 to 2,000 (cfs/hr) for moderate and very high flows. The presence of the dams made the upstream gages a poor predictor of future conditions at Seguin. In the end, the predicted and measured rainfall in the watershed was used to make a decision about the timing of sampling trips.

3.4 Data collection methods

The data collected during sampling trips for all eight of the USGS gage stations included: cross section surveys, bed sediment samples, and suspended sediment concentration samples at low flow. At the Seguin station, bed load and suspended load were measured over a range of flow conditions. The Seguin site was selected for measurement of bed and suspended load for four reasons. The first was that the stations is the most upstream gage in the study reach. Therefore, obtaining measurements of sediment transport rates at the upstream location would allow for the rating curves developed from the data to be used as upstream boundary conditions on any future modeling efforts of the reach. The second reason that the site was chosen was very pragmatic. It was simply the easiest of all of the sites to make bed load measurements at. The Sequin site had a bridge deck that was much closer to the water than the other three sites and had lower automobile volume and speed limits. Additional reasons that led to the selection of Seguin included less public recreational use and no tidal influence.

Suspended sediment samples at the Seguin site were initially attempted with a Federal Interagency Sedimentation Project (FISP) depth-integrated sampler (US DH-2TM bag-type) and the Equivalent Width Increment (EWI) method (Diplas et al., 2008). The US DH-2TM bag-type sampler is designed to collect 1 L isokinetic samples in depths up to 35 ft and velocities in the range of 2.0 to 6.0 ft/sec. The sampler was lowered and raised using a three-wheel truck USGS Type A crane with a B-56M sounding reel. We have used this sampler on the Brazos and Trinity rivers in Texas, and a major problem we have encountered is that the sampler does not reliably collect water samples at low flow conditions. At the Seguin site, we were not able to get reliable samples of the suspended sediment using the DH-2TM under any of the flow conditions. Because of this, suspended sediment samples were collected with a bucket attached to a rope. The bucket was allowed to fill with water, sink, and be dragged to some extent by the flow. It was then gently raised back to the bridge deck. Samples were collected across the channel in equal width intervals and then integrated together to produce a single sample per flow condition and sampling day.

Bed load measurements were made at Seguin using a custom-built Helley-Smith (HS) sampler. The sampler had a 3 in x 3 in opening with a 7.5 x 4.3 in flared diffuser where a mesh sample collection bag was attached (figure 3.1A). The size of the sampler opening was based on an initial bed particle size distribution that showed that $d_{max} < 100$ mm and $d_{50} = 20$ mm. The Sequin bridge deck is relatively close to the bed of the river. Because of this, we opted to control the sampler using a long steel pole attached to the mouth of the sampler rather than attaching

the sampler to a cable and reel (figure 3.1). The steel pole was designed to be modular to allow for easier transport and adjustment of the length as needed. Collection bags for the sampler were made out of 0.25 mm opening cloth mesh (figure 3.2). Bed load samplers were collected over two minutes at 16 equally spaced width intervals across the channel. The short sampling time for each sample was done to minimize the total time it took to sample the entire channel width following the recommendations for flashy rivers of Francalanci et al. (2013). All bed load samples from each width increment were combined to provide a single representative bed material sample for the cross section at each flow condition.

Figure 3.1: Primary sampling equipment. (A) The Helley-Smith sampler; (B) the sampler with 6 poles attached; and (C) deployment of the sampler from the bridge deck.

Figure 3.2: Mesh bag used for collecting HS bed sediment samples.

An attempt was made to supplement the Helley-Smith bed load measurements with two additional measures of bed sediment mobility. The first was through the placement of buried bucket samplers at the Seguin, Gonzales, and Cuero sites. The second was the use of radio frequency identification (RFID) tagged particles at the same three sites. The purpose of the buckets was to trap gravel traveling as bed load during large flow events. The sizes of the trapped material would then provide a point of comparison with the HS samples to ensure that the HS sampler was capturing all of the sizes in motion. The amount of sediment in the bucket could also be used to make rough estimates of the total mass moved during the event. Unfortunately,

none of the buckets could be located after the first high flow event (3.3). Because the Gonzales and Cuero are fairly high-use recreational areas, we suspect that the buckets were removed by people wandering through the river at these sites. The same is possible at Sequin. However, because the bed sediment at Sequin is smaller, it is possible that general movement of the bed at the site led to dislodgment of the bucket by natural processes. In any event, the buckets did not yield any usable data.

Figure 3.3: (A)Installed bucket in Gonzales at 07/04/14; (B) Removed and missed bucket.

The purpose of the RFID tagged particles was to identify the sizes in motion during a given flow. Each RFID tag is associated with a unique digital number that can be detected by an antenna and reader. Therefore, if the size and location of a given particle is linked with its RFID, repeat scans of tagged particles present before and after a major flow event can be used to determine the size of grains in motion during the flow event. Two sizes of RFID tags were used. The larger (32 mm) emit a stronger signal when activated by the antenna and are therefore easier to find. However, these larger tags are also too large to be placed in many of the particles at Seguin site. For this reason, we also used smaller (23 mm) tags. Inserting the tags into gravel collected at each of the three upstream stations was not trivial. Use of masonry drill bits and rotary hammers quickly fractured all but the largest stones. This was especially true when attempting to drill into the very prevalent chert grains. To overcome the fracturing issue, we used a table saw to cut a slot in the smaller grains deep and wide enough to accommodate the tags (figure 3.4A). The tags were then placed in the slot and packed with epoxy to secure them in place (figure 3.4B). Once the tags were in place, each stone was sized, weighed, and scanned to associate it with the RFID. The stones were then placed at the gage site during low flow.

Water samples were processed in the laboratory to obtain the average suspended sediment concentration, C, associated with each discharge at the time of sampling. Measurements of the total suspended sediment concentration were obtained through filtering for the lower concentration sample following the ASTM standards outlined in ASTM D3977 - 97(2007) (ASTM, 2007). For higher concentrations, the entire water and sediment mixture was placed in pre-weighed pans. The pans were then placed in an oven at low temperature to remove all of the water through evaporation. Following several days in the oven, the pans were reweighed to allow for calculation of the total suspended sediment mass. During low flows, the amount of

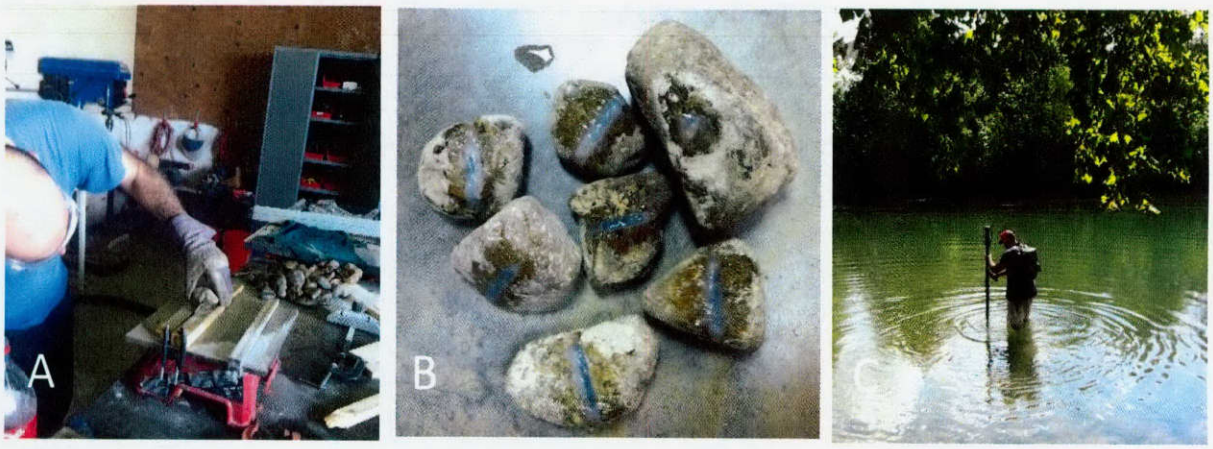

Figure 3.4: (A) Cutting the RFID tag slots in stones from the river bed; (B) stones with embedded RFID tags; (C) Placing tagged stones and scanning with the RFID antenna at the Seguin station during low flow.

suspended material captured was too low to allow for sizing of the material with the Malvern Mastersizer. In these cases, the wash load percentage was measured by running the well-mixed water column samples through a 63 μm small sieve. The ratio of the passed sediment weight through the sieve over the remained sediment weight on the sieve shows the percentage of the suspended sediment smaller than 63 μm which is considered as wash load. Bed material and bed load samples were both sized through standard drive sieving to produce a percent finer than by weight grain size distribution.

4 Data

4.1 Summary of flow conditions captured

The sampling portion of the project ran from January 1, 2014 to April 30, 2015. Cross section geometry and bed sediment grain size data was collected at all 8 USGS gage stations. At Seguin, five bed load samples were collected over the largest range of flow conditions possible. Flows below the smallest discharge sampled did not produce motion, and flows larger than the highest sampled were dangerous to collected data on as the water was nearing the bridge deck. The largest flow event to occur during the sampling period in Seguin took place during the last week of April 2015. A summary of the bed load and suspended load samples collected at Seguin under low, moderate, and high flow conditions is given in Table 4.1.

# of bed load Samples	# of suspended Samples	Relative Flow Magnitude	Flow Exceedance Condition
5	5	High	Q exceeded $\leq 20\%$
-	1	Moderate	$20\% \leq Q$ exceeded $\leq 50\%$
-	2	Low	$50\% \leq Q$ exceeded $\leq 90\%$

Table 4.1: Sampling conditions for USGS gage station near Seguin.

4.2 Notes on measured data

Summary figures of the collected data are shown below figures 4.1-4.8, and all collected data is listed in table 4.2. Discharges shown in the figures and tables are the 15-minute USGS instantaneous discharges. We use the 15-minute USGS data throughout the analysis because the river is flashy, and use of the daily mean values tends to smooth over true peaks in discharge. In the summary figures, Q_b is the measured bed load transport rate, C_{ss} is the total suspended solids concentration, and C_{SBM} is the suspended bed material concentration ($d > 63$ μm). All cross sectional data was surveyed at low flow conditions.

Figure 4.8 shows the overall downstream trends for drainage area, slope (discussed in detail in the next section), active channel width, bankfull depth, return period flows at 1.5, 2, and 10 years, and the average bed material grain size statistics. As expected, channel width and depth both slightly increase in the downstream direction. Grain size drops off significantly at Victoria where the river transitions from a gravel bed river to a tidally influenced sand bed reach.

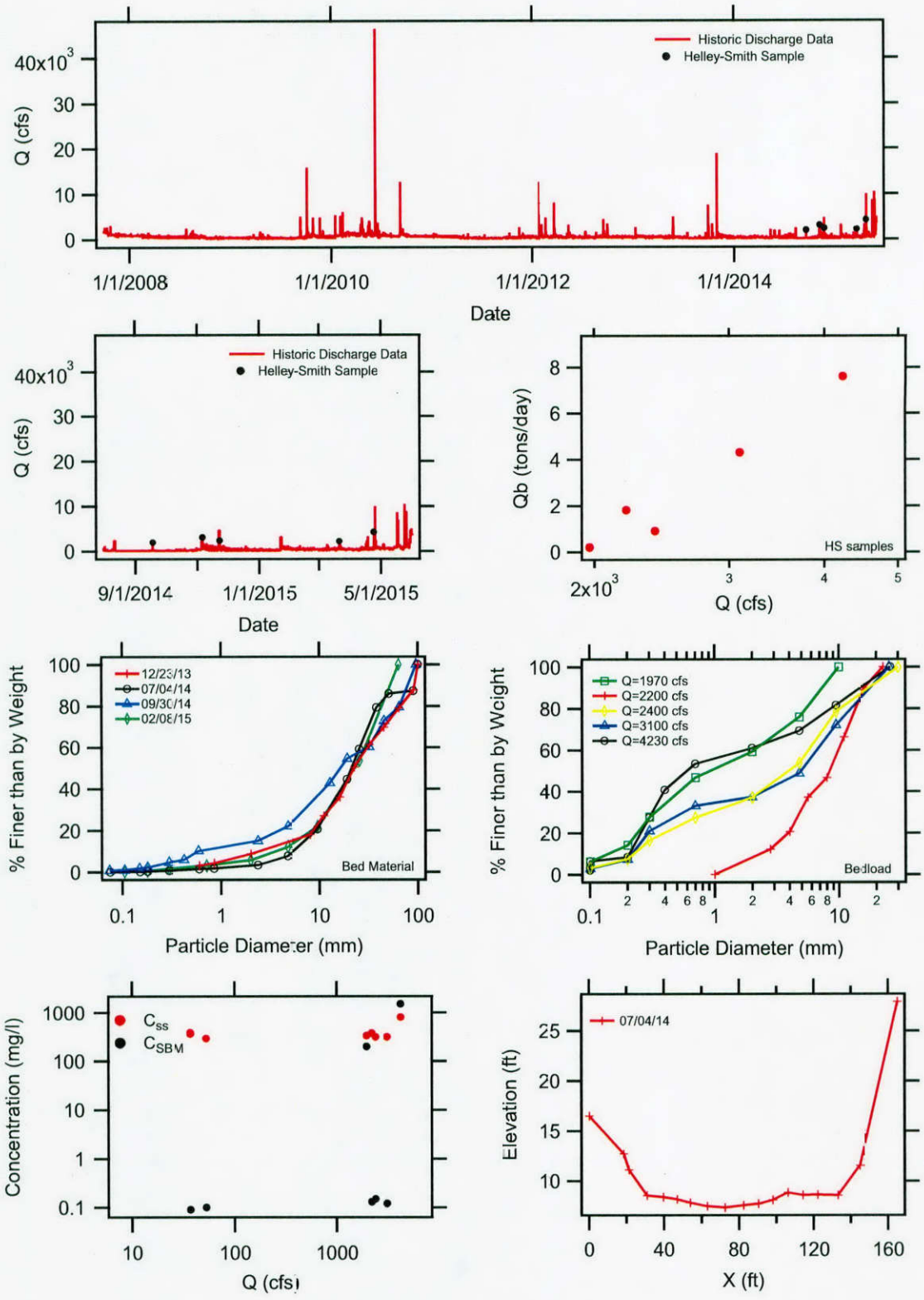

Figure 4.1: Summary of collected data at Seguin (USGS gage 08169792).

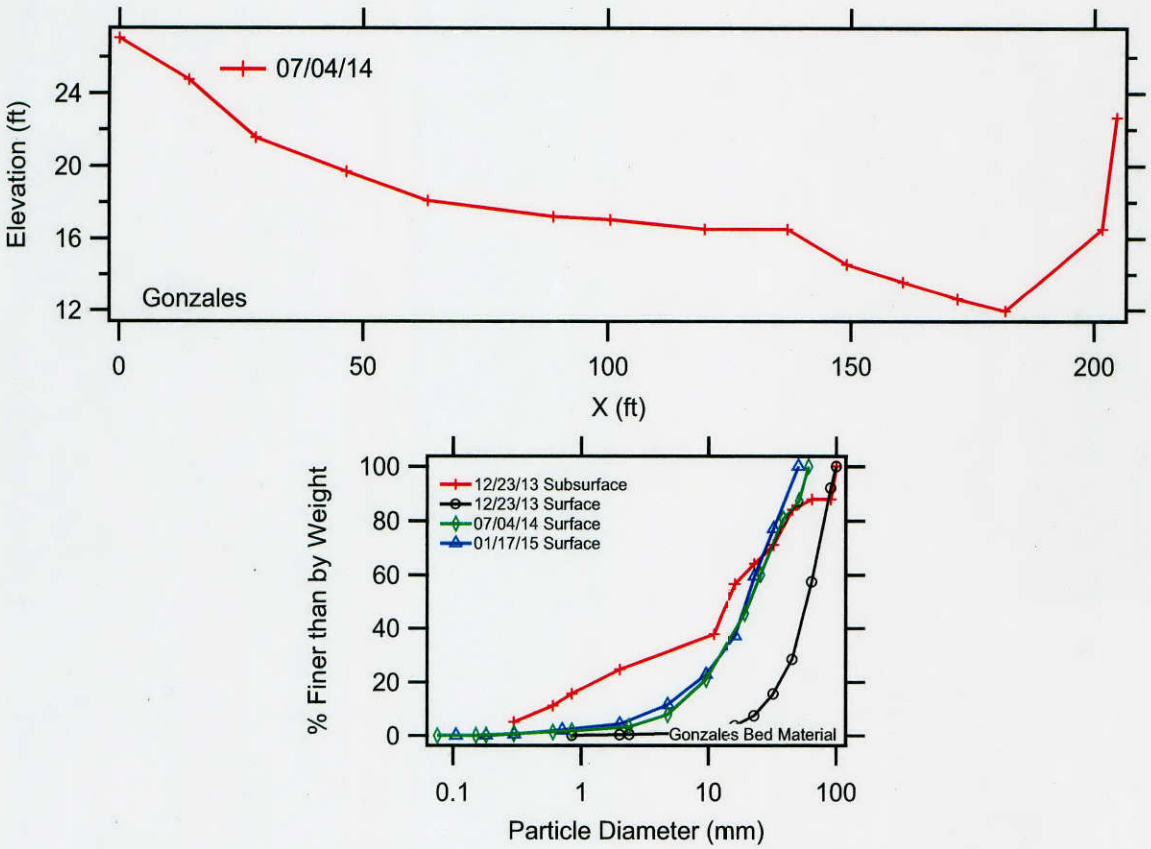

Figure 4.2: Summary of collected data at Gonzales (USGS gages 08173900).

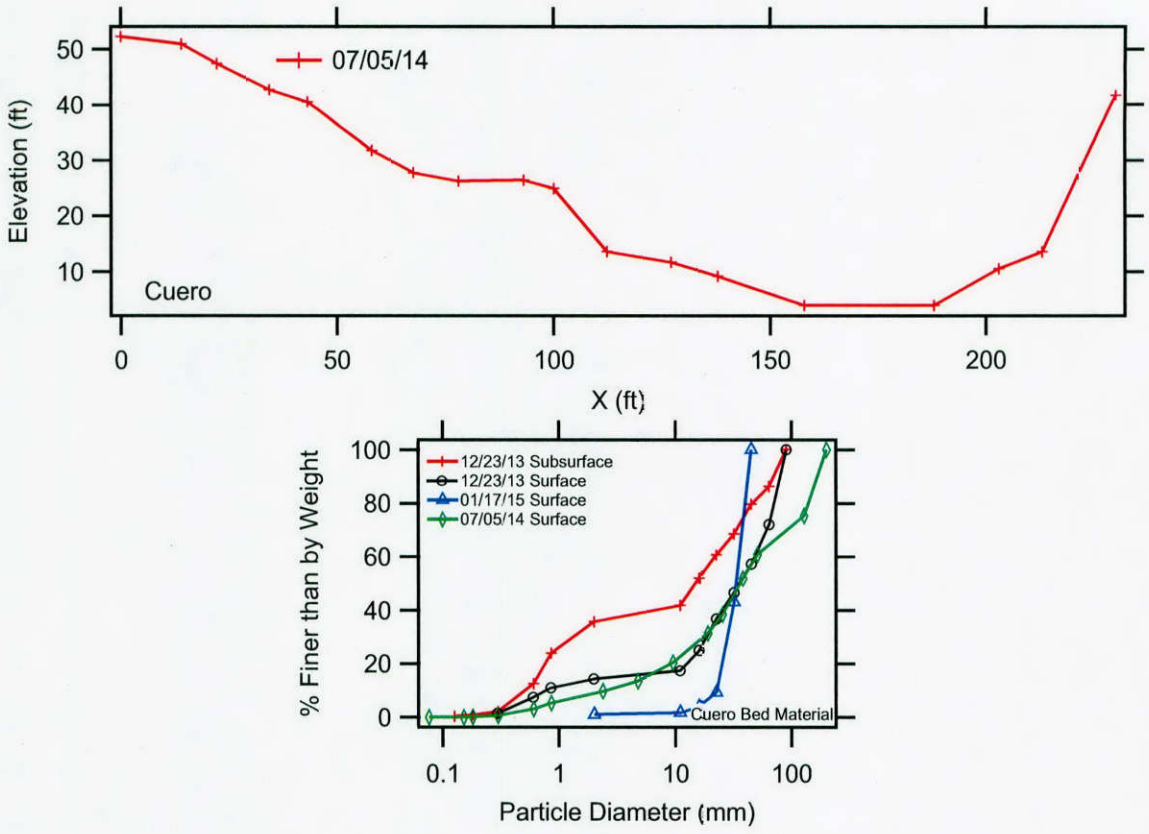

Figure 4.3: Summary of collected data at Cuero (USGS gage 08175800).

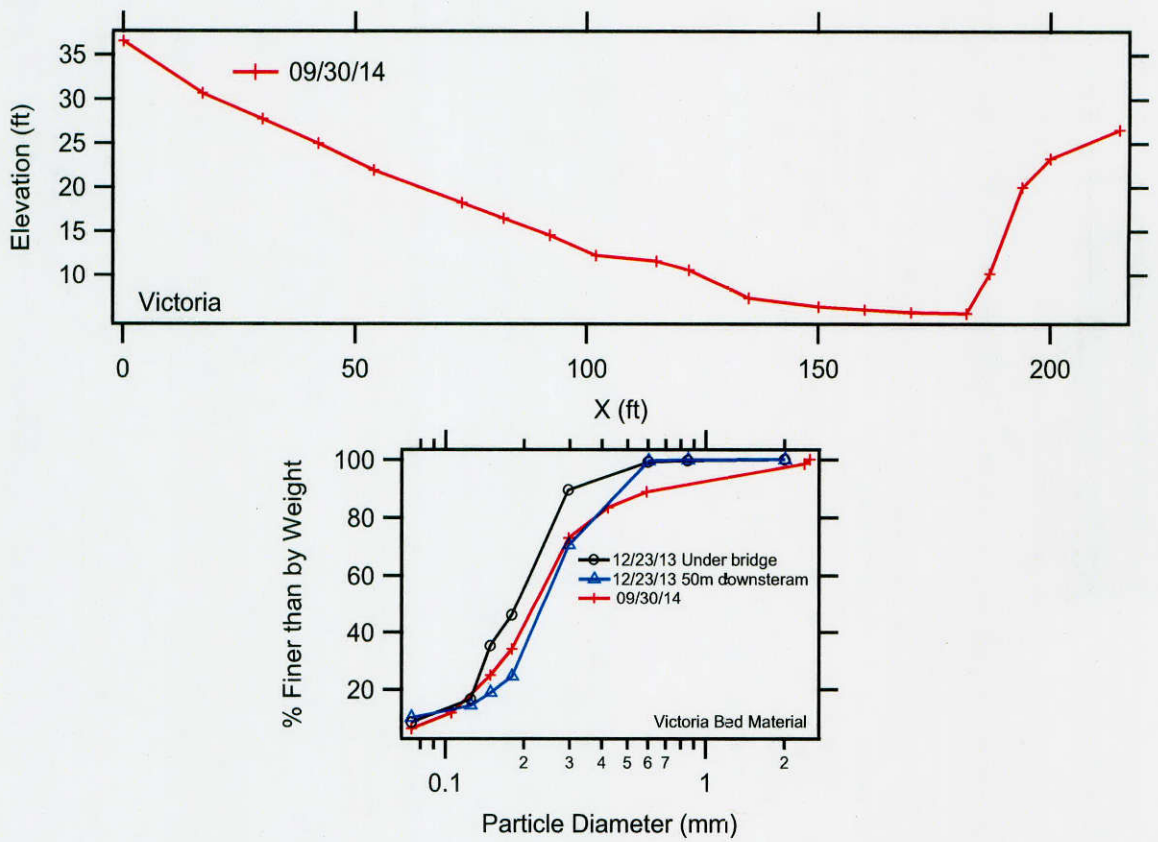

Figure 4.4: Summary of collected data at Victoria (USGS gage 08176500).

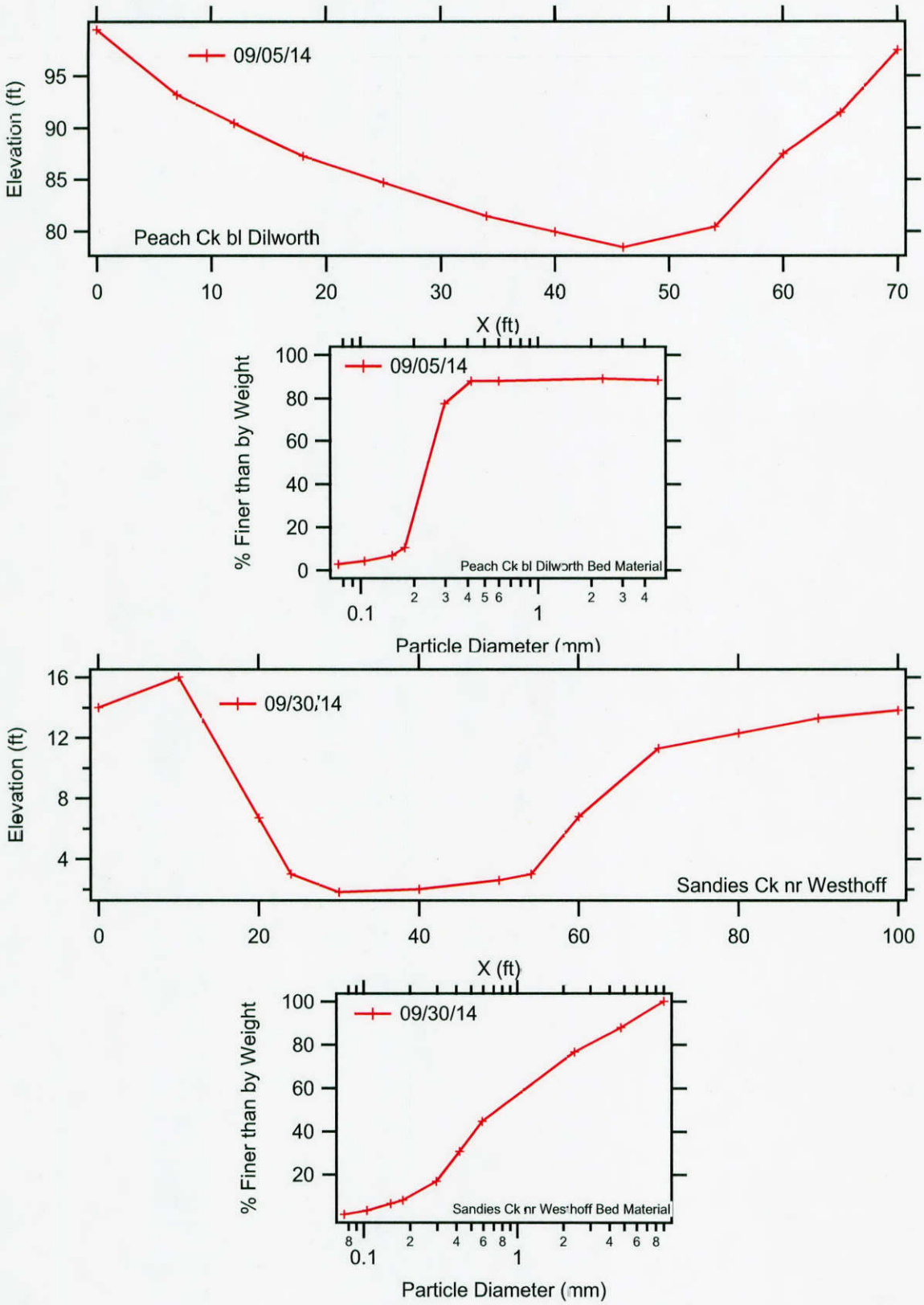

Figure 4.5: First figures of data collected on tributaries to the lower Guadalupe River.

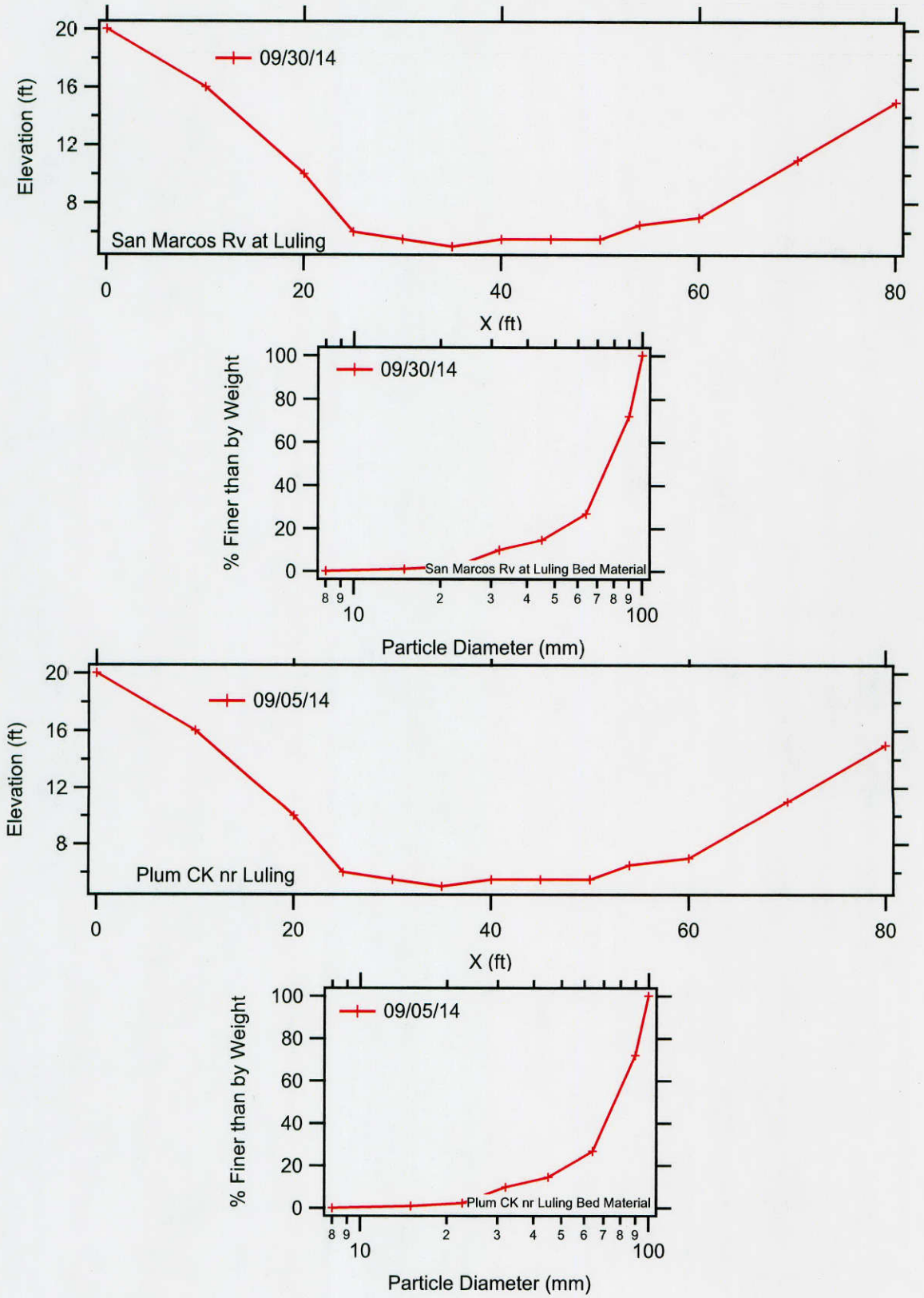

Figure 4.6: Second figures of data collected on tributaries to the lower Guadalupe River.

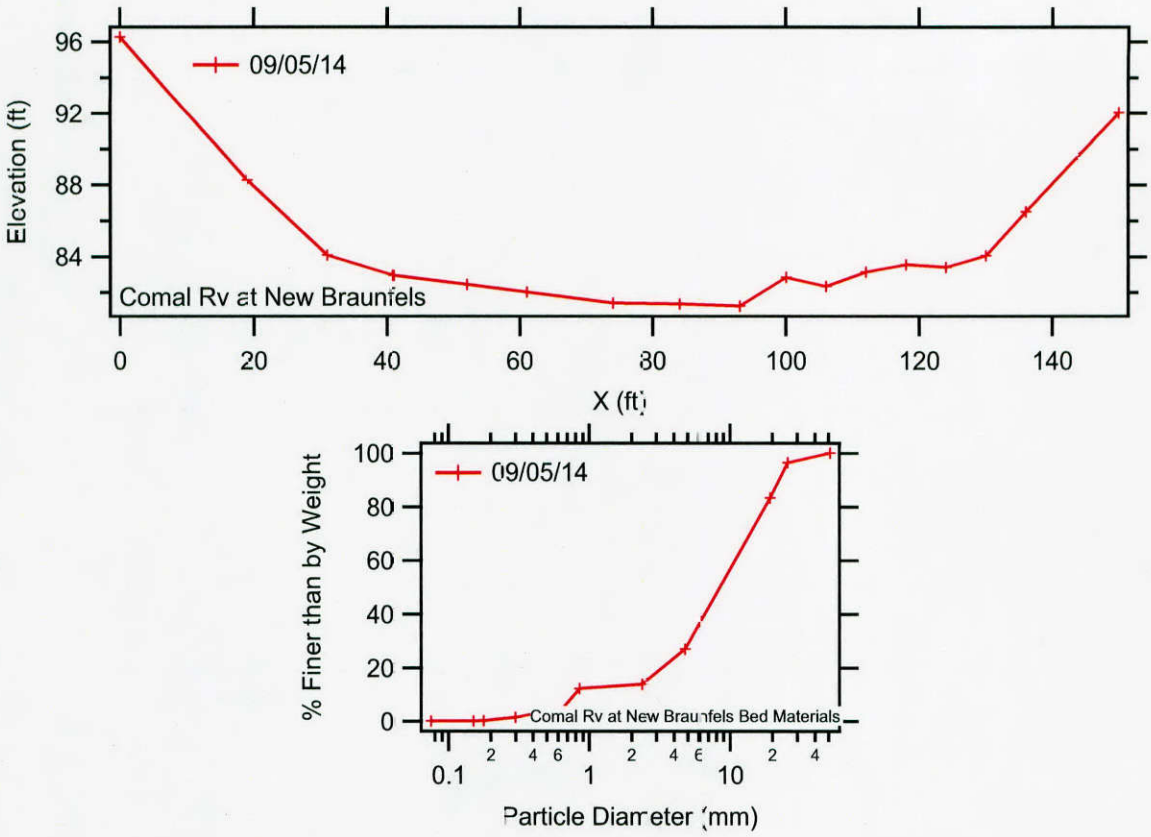

Figure 4.7: Third figures of data collected on tributaries to the lower Guadalupe River.

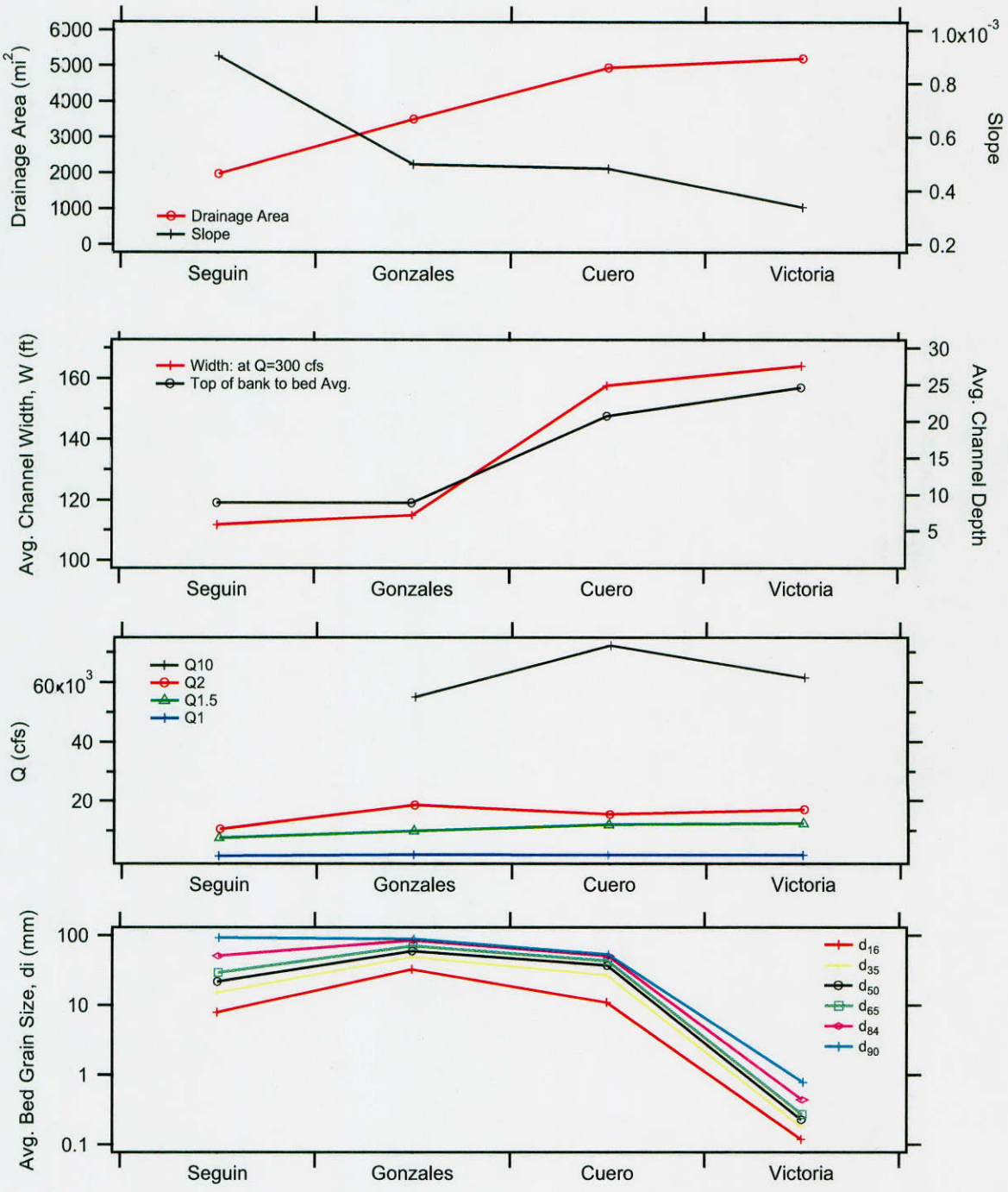

Figure 4.8: Downstream trends in major stream properties. Average bed grain sizes are based on surface layer samples.

Site	Date	Condition	Location on Hydrograph	Bed Size Measured? (Used)	Bed Load Measured?	Q [cfs]	R_h [ft]	U [ft/s]	Grain Size Statistics					Bed Load [tons/day]	Wash Load [%]	Total SSC [g/l]
									Material	d_{16} [mm]	d_{50} [mm]	d_{84} [mm]	d_{90} [mm]			
Seguin	12/23/13	Moderate	Falling	Yes	No	497	4.93	0.8	Bed	6.78	22.00	79.51	92.00	-	-	-
Seguin	7/4/14	Low	Base	Yes	No	135	4.06	0.3	Bed	7.82	21.43	47.20	92.11	-	-	-
Seguin	8/21/14	Low	Base	No (7/4/14)	No	37	3.70	0.1	Bed	7.82	21.43	47.20	92.11	-	100	0.38
Seguin	9/18/14	High	Rising	No (7/4/14)	Yes	1970	6.49	2.0	HS Sample	0.19	1.05	6.52	7.83	0.2	99.4	0.33
Seguin	9/30/14	Low	Base	Yes	No	53	3.80	0.1	Bed	2.70	16.60	70.85	79.90	-	100	0.29
Seguin	11/6/14	High	Peak	No (9/30/14)	Yes	3100	6.85	2.7	HS Sample	0.25	5.02	16.28	19.70	4.30	100	0.31
Seguin	11/23/14	High	Falling	No (9/30/14)	Yes	2400	6.96	2.2	HS Sample	0.29	4.13	14.62	20.39	0.90	100	0.31
Seguin	1/17/15	Low	Rising	No	No	37	3.70	0.1	Bed	7.82	21.43	47.20	92.11	-	100	0.36
Seguin	2/8/15	Low	Falling	Yes	No	300	4.14	0.6	Bed	6.63	23.62	50.05	54.91	-	-	-
Seguin	3/21/15	High	Peak	No (2/8/15)	Yes	2200	6.62	2.2	HS Sample	3.34	8.53	14.75	16.04	1.80	100	0.37
Seguin	4/24/15	High	Peak	No (2/8/15)	Yes	4230	8.35	3.1	HS Sample	0.23	0.63	11.67	17.04	7.60	98.1	0.79
Gonzales	12/23/13	Moderate	Rising	Yes	No	590	2.56	3.6	Bed	32.44	59.12	83.92	88.42	-	-	-
Gonzales	7/4/14	Moderate	Rising	Yes	No	590	2.56	3.6	Bed	7.72	21.04	44.35	52.70	-	100	0.35
Gonzales	8/21/14	Low	Base	No (7/4/2014)	No	173	2.14	1.4	Bed	7.72	21.04	44.35	52.70	-	99.2	0.39
Gonzales	1/17/15	Moderate	Rising	Yes	No	300	2.34	2.1	Bed	6.68	19.80	37.44	42.15	-	100	0.40
Cuero	12/23/13	Moderate	Base	Yes	No	537	4.09	1.9	Bed	7.07	36.12	75.10	80.69	-	-	-
Cuero	7/5/14	Moderate	Base	Yes	No	302	3.75	1.3	Bed	6.46	36.40	153.51	170.94	-	100	0.29
Cuero	8/21/14	Low	Base	No (7/5/14)	No	111	3.37	0.6	Bed	6.46	36.40	153.51	170.94	-	100	0.32
Cuero	1/17/15	Moderate	Rising	Yes	No	480	4.02	1.4	Bed	24.46	33.59	41.35	42.72	-	100	0.51
Victoria	12/23/13	Moderate	Base	Yes	No	476	3.61	1.9	Bed	0.12	0.19	0.28	0.31	-	-	-
Victoria	9/30/14	Moderate	Base	Yes	No	220	2.74	1.3	Bed	0.12	0.23	0.44	0.79	-	-	-

Table 4.2: Summary table of the data collected at the four main gaging stations.

Site	Date	Bed Material[mm]				Wash Load	Total SSC
		d_{16}	d_{50}	d_{84}	d_{90}	[%]	[g/l]
San Marcos River at Luling	09/30/14	9	32	88	96	100	0.36
Plum Ck near Luling	09/05/14	47	77	94	96	100	1.5
Peach Ck bl Dilworth	09/05/14	0.16	0.22	0.25	0.32	100	0.65
Sandies Ck near Westhoff	09/30/14	0.28	0.88	4	6	100	2.2
Comal River at New Braunfels	09/05/14	3	11	19	22	100	0.31

Table 4.3: Summary of tributary data.

4.3 Bed Load Data

Bed load data was collected with the HS sampler at five different flow conditions ranging from Q = 1,970 cfs to Q = 4,200 cfs. At Q = 1,970 cfs, only 0.3 lbs of material was collected over a total sampling period of 32 minutes. Based on this measurement, and the measurement at Q = 2,200 cfs, a practical discharge value for the onset of measurable transport rate at the station is Q = 2,000 cfs.

Two general trends are observed in the bed load data with increasing discharge. The first is that the bed load mass flow rate is proportional to Q^{β} (figure 4.1). The second is that the size distribution of the material captured with the sampler fines with increasing discharge when data from Q = 1,970 cfs is excluded (figure 4.1). The reason for this is that the sampler captured an increasingly larger fraction of sand as discharge increased.

4.4 RFID tags

RFID tags were placed in the three upstream gravel bed stations of Seguin, Gonzales, and Cuero on 21 August 2014. Unfortunately, none of the sites were originally scanned immediately after placement of the particles. All initial scans took place after the particles had been in the field for some time. At Seguin, scans were conducted after flow events of Q = 2,500 cfs and Q = 4,700 cfs (Table 4.4). Only one scan was performed at Gonzales and Cuero approximately 5 months after deployment of the RFID particles (Table 4.4). Flow during the time period of deployment at these two sites was very mild and no useful data was obtained from the RFID tagged particles at these sites. The data from the Seguin site was somewhat better, and suggests that particles less than approximately 45 mm in diameter were possibly in motion during the 4,700 cfs event. However, the data that led us to this results was not conclusive. A more nuanced discussion on the findings is presented below.

At Seguin, the scan on September 30th 2014 (approximately one month after the original placement) showed that a significant number of the originally placed stones were not detected by the antenna. Particles missing in the scan were some of the largest RFID tagged particles, reaching up to the 6 to 9 cm range (figure 4.9). Calculations we performed to estimate the possible range of particle sizes in motion between the scan dates, along with our bed load measurements, both suggest that movement of particles in the 6 to 9 cm range at a discharge of 2,500 cfs was unlikely. We suspect that the missing larger particles were due to either burial of

Station	Date of RFID placement	Scan date	Q_{max} [cfs]	Date of Q_{max}
Seguin	8/21/2014	9/30/2014	2500	9/18/2014
	8/21/2014	2/8/2015	4,700	11/22/2014
Gonzales	8/21/2014	1/17/2015	2,120	11/24/2014
Cuero	8/21/2014	1/17/2015	1,620	11/25/2014

Table 4.4: Summary of the placement of the RFID tags

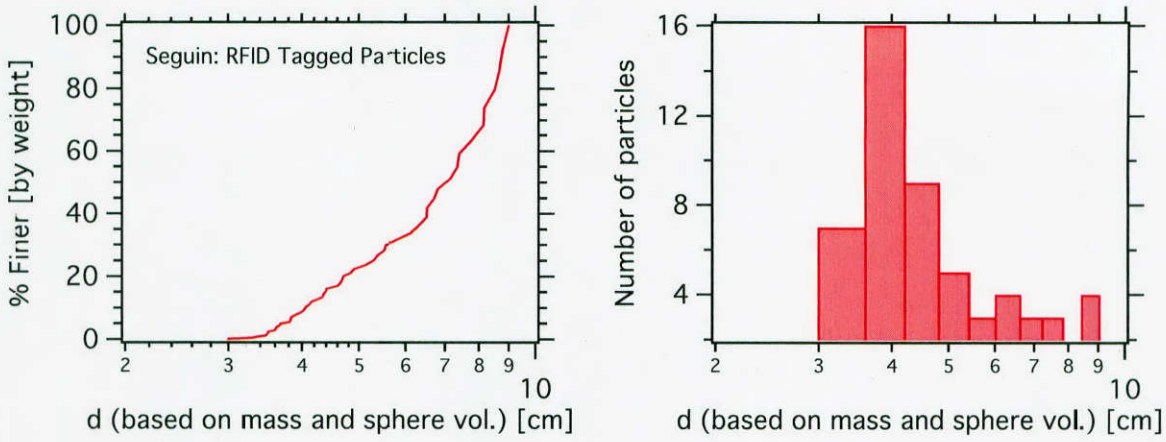

Figure 4.9: Size statistics for the tracers deployed at Seguin. The figure on the left shows the cumulative percent finer than by weight size distribution and the figure on the right shows the frequency distribution of particle sizes. The size, d, was obtained by weighing each grain and then back calculating an equivalent spherical diameter assuming a specific gravity of 2.65.

the original tracers by upstream sediment that moved in under the 2,500 cfs flow, or human intervention. The larger particles were visible through the shallower parts of the stream and it is possible that they caught the eye of swimmers or fishermen.

The second Seguin scan was carried out on February 8, 2015 following a high flow condition of 4,700 cfs. Bed load measurements using the Helley-Smith sampler were made during this event but at a discharge slightly less than the peak, i.e., at 4,230 cfs. Results from the scan were difficult to reconcile with those of the first scan on 9/30/2014. Some particles that had not shown up in the first scan were present in the second scan. There were no size preferences with these"reappearing" particles; that is, some tagged particles from all size classes that were absent in the first scan showed up in the second scan. One possible explanation for the observations is that the particles that showed up as "missing" on the first scan were buried by fresh deposits during the 2,500 cfs event and then re-exposed to the surface during the 4,700 cfs event. The section of river where the tracers were placed was downstream of the road crossing in section of slight channel expansion. The presence of a medial bar suggests that the section can experience preferential deposition of material transported through the road cross section. Another explanation is simply that the scanner was not working properly during one or both of the scans.

While some particles that were not present in the first scan reappeared in the second, there were other particles that were present in the first scan but then absent in the second. Possible explanations for this are: (1) that the scanner was not working properly, (2) that the missing particles were buried, or (3) that the missing particles were entrained and transported down channel. Particles present in the first scan but absent in the second tended to be biased toward the smaller size fractions of placed tracers. Most of them fell below a square sieve opening of 4.5 cm; though a few measured between a 4.5 and 6.4 cm square opening. While being subjective, our interpretation of the second scan data is that the 4,700 cfs flow was able to move particles that can pass through a 4.5 cm sieve size opening. A simple critical shear stress analysis based on reach-averaged hydraulics and a τ^*_{cr} ranging from 0.03 to 0.06 without accounting for hiding also suggested that the flow should have been able to move particles as big as 2 to 5 cm in diameter.

5 Analysis and Results

5.1 Sediment rating curves and transport calculations

The sediment load rating curves (i.e., equation 2.3) were developed using measured transport data from the Seguin station and calculated transport rates at the remaining three stations.

Water column samples from Seguin suggests that the suspended bed material load was negligible in the study reach at the time of sampling (Table 4.2). Therefore, at Seguin, the measured bed load, Q_b was used solely to construct the sediment load rating curve and histogram. Two different total load rating curves were produced using the data. The first includes the low-transport condition at Q = 1,970 cfs. In the second, the data from Q = 1,970 cfs was excluded (figure 5.1). The reason for this exclusion was that the bed load sample at Q = 1,970 cfs was very small, making us suspect the appropriateness of the sampler at this near critical condition (Bunte et al., 2008). Additionally, the regression analysis is quite sensitive to inclusion or exclusion of this point. Including the point results in a rating curve power of $\beta = 4.3$, while excluding it results in a value of $\beta = 2.8$ (table 5.1). Because the entire effective discharge calculation method is controlled by the flow frequency histogram and the slope of the rating curve, i.e. β, inclusions or exclusion of the bed load measurement at Q = 1970 cfs will ultimately dictate the value of the Q_e. For our final effective discharge calculation, we reason that the rating curve developed excluding the low-flow condition is the most appropriate. This will be discussed in more detail later on. Also, because of the increasing sand load observed in the Helley-Smith samples, the total bed load transport rate was decomposed into a gravel and sand load component, $Q_b = Q_{b,gravel} + Q_{b,sand}$. The rating curves associated with each of these fractions is also shown in figure 5.1 and Table 5.1.

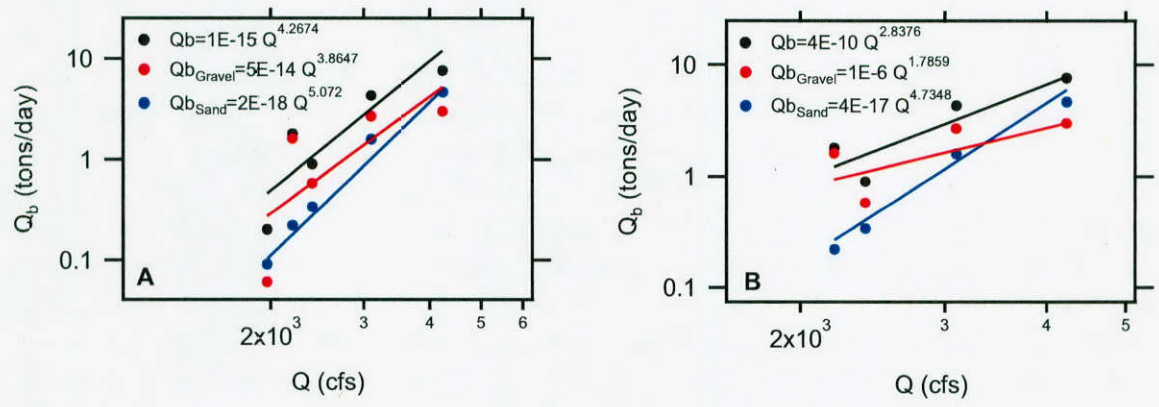

Figure 5.1: Seguin measured bed load rating curves for two conditions of (A) including all the 5 measurements; (B) including 4 measurements and neglecting the sample collected at minimum discharge close to incipient motion.

For the Gonzales, Cuero, and Victoria stations, measured grain size distributions and cross sectional geometries were used along with SAMwin to calculate the sediment load rating

Condition	Sand and Gravel		Sand		Gravel	
	α	β	α	β	α	β
Including Q_b @Q = 1970 cfs	1.00E-15	4.2674	8.00E-19	5.072	2.00E-14	3.8647
Excluding Q_b @Q = 1970 cfs	**1.00E-10**	**2.8376**	1.00E-17	4.7348	4.00E-07	1.7859

Table 5.1: Bed load rating curve coefficients for Seguin station differentiated for sand, gravel, and mixture of sand and gravel. Bolded values are those used in the effective discharge calculation.

curves. The bed load and total bed material load rating curves were developed by calculating the load in tons per day associated with the daily discharge data at the time of sampling. The paired data was then fit with a power law curve to produce the rating curve. Additional data required by SAMwin for the calculations includes the local reach slope. Slope measurements were not made at the time of sampling because the surveying equipment available to us (construction level and tape) was not accurate enough to measure the small slopes on the Guadalupe. For this reason, values of S were obtained from a USGS database of computed slopes for Texas gaging stations and some additional analysis.

Station	USGS	Based on the	Google Earth	
		Manning Eq.	Land	Bank
Seguin	-	0.00022	0.0009	0.0005
Gonzales	-	-	0.0005	0.0002
Cuero	0.000482	-	0.0004	0.0004
Victoria	0.000339	-	0.0003	0.0002

Table 5.2: Slope calculations for Seguin and Gonzales

The USGS computed slope used in the analysis is referred to as the "main-channel slope" by Asquith and Slade (1997). The main-channel slope is defined as the change in elevation between the two end points of the main-channel divided by the distance, L (Asquith and Slade, 1997). In the calculation method, L is the longest defined channel shown in a 10-meter digital elevation model (DEM) from the approximate watershed headwaters to the point of interest, and the elevation change between the two points is extracted directly from the 10-meter DEM. The main-channel slope is therefore more of a watershed slope based on the channel network than it is a local reach slope. Because of its calculation method, we suspect that the main channel slope values are, on average, slightly higher than the local reach slopes at each station. Our reasoning is that the main channel slope by definition incorporates elevation change further up in the watershed where slopes are likely higher. Nevertheless, this definition of slope was very reasonable for Cuero and Victoria. The slopes of Seguin and Gonzales were not available in the USGS computed slopes data base. Therefore, slope was estimated using Google Earth images and the elevations of the river bank and adjacent land. Table 5.2 shows a summary of calculated slopes. We also estimated the slopes using the measured cross sectional geometry during the time of sampling and the USGS 15-min discharge data. Using this data, a slope was calculated for each flow condition using the Manning equation and assumed n values ranging from 0.03 to 0.04. Based on these analyses, we have selected slopes of $S = 0.0009$ at Seguin and $S = 0.0005$

at Gonzales. for the transport calculations. These values seem to be reasonable given that the downstream slope at Cuero and Victoria are $S = 0.000482$ and $S = 0.000339$ respectively.

Several different transport equations were used to develop the rating curves. Some are for bed load only, while others are for total load. A list of all of the power-law coefficients for the rating curves developed for each station are listed in table 5.3.

Station	Bed	Rating Curve Coeff.	MPM $[Q_b]$	Schoklitsch $[Q_b]$	Yang $[Q_{tl}]$	Ackers White $[Q_{tl}]$	Engelund Hansen $[Q_{tl}]$	Einstein $[Q_{tl}]$
Seguin	Gravel	α	0.0208	0.0001	0.0009	0.0002	-	-
		β	1.308	1.6881	1.6407	1.7388	-	-
Gonzales	Gravel	α	0.0004	1E-06	**2E-05**	2E-06	-	-
		β	1.3021	1.7311	**1.6205**	1.7238	-	-
Cuero	Gravel	α	0.0794	0.0026	**0.003**	0.0023	-	-
		β	1.057	1.3023	**1.4992**	1.4765	-	-
Victoria	Sand	α	-	-	**0.02**	0.0029	0.0232	0.0022
		β	-	-	**1.5183**	1.9337	1.5729	2.0504

Table 5.3: Calculated rating curve coefficients for main gaging stations of Guadalupe River based on measured cross section and grain size distribution along with SAMwin model. Bolded values are those used in the effective discharge calculation for the three downstream stations.

5.2 Effective discharge calculations

5.2.1 Development of the flow PDF

Histogram estimates of the discharge pdfs at each station were developed using both daily and 15 min discharge data available from the USGS NWIS. Both the Cuero and Victoria stations have over 50 years of daily flow data. However, at Gonzales, data is only available from 1997 onwards, and the Seguin gage has only been in operation since 2005. Therefore, for the daily flow analysis, data from 1/1/1997 to 12/31/2015 (19 years of data) was used for Gonzales, Cuero, and Victoria; for Seguin, we simply used the longest range of available data which spanned from 3/15/2005 to 12/31/2015 (approximately 10.75 years of data). For the 15 min data, we used all of the available data at all four stations, which spanned from 10/1/2007 to 12/31/2015 (approximately 8 years).

We developed the flow histograms using only discharges greater than 2,000 cfs at the first three stations. This was done for two reasons. The first is that the three upper stations have gravel beds that do not see significant motion at flows less than 2,000 cfs. Therefore, removing discharges less than 2,000 cfs is a way of adding in a critical-condition concept in the development of the sediment load histograms. The other reason for removing the smaller discharges is that if discharges less than 2,000 cfs are kept in the analysis, the peak in the sediment load histogram sometimes occurs in the second bin ($Q = 1{,}125$ cfs) at Gonzales and Cuero; even though we suspect that bed is quite stable at these discharges. All discharges were kept in the analysis for the Victoria site since the bed is composed of sand and likely in motion at flows less than 2,000 cfs.

All flow histograms, except the daily flow histogram for the Seguin site, were developed using a bin width of 750 cfs. This bin width was selected by trial and error as one that was able to adequately describe the shape of the sediment load histogram for flows less than 20,000 cfs. A bin width of 200 cfs was used for the Seguin daily flow histogram because of the relatively small number of flows greater than 2,000 cfs in the daily data. The bin width was re-set to 750 cfs at Seguin for the 15 min data.

5.2.2 *Sediment transport effectiveness distributions*

Effective discharge estimates, Q_e, were made directly from the sediment load histograms, S_h (Wolman and Miller, 1960), that were developed using the flow-frequency histograms and rating curves. The S_h distributions were created by multiplying the rating-curve derived load associated with each bin-centered discharge with the flow-frequency data in that bin (equation 2.2):

$$S_h = Q_s f_Q \tag{5.1}$$

were Q_s is the total bed material transport rate (both bed and suspended load) obtained from the site rating curves using the bin-centered discharges. For Seguin, the rating curve used was based on the measured bed load. For the remaining three sites, we used the rating curves that were developed using standard sediment transport relations and the measured cross sections and grain size distributions. The coefficients for all of the developed rating curves can be found in table 5.3. All of the transport equations used produced similar β values, ranging from 1 to 2, and therefore they all resulted in similar effective discharge estimates. Of all the equations used in development of the rating curves, the Yang total load equation was selected as being the most appropriate for all three stations since the Yang equation was developed using both gravel and sand. Figures 5.2 shows the sediment load distributions using the daily flow data, and figure 5.3 shows the analysis based on the 15 min data.

5.2.3 *A note on picking the effective discharge*

The effective discharge is defined as being the discharge associated with the peak or highest value of S_h. However, S_h does not monotonically increase from zero up to the peak value and then monotonically fall back down to zero with increasing discharge as conceptualized in figure 2.2 and in Wolman and Miller (1960) at all four of the stations. Sometimes, the maximum value of S_h is a lone, isolated bin. Often times, this lone peak occurs in one of the first few bins, and selection of such a discrete peak would lead to effective discharges associated with the lowest flows in the river. Additionally, the problem of an isolated peak can come and go depending on the exact number of bins and bin widths used; making the selection of effective discharge vary dependent on the method used for generating the discharge pdf.

To avoid the lone-peak problem, we have followed the suggestion of Biedenharn et al. (2000) by fitting a smooth and continuous line through the entire S_h distribution by eye. The effective discharge is then chosen as the peak of this smooth distribution. While this method does retain a measure of user subjectiveness, the method does produce more consistent results for the effective discharge, and it keeps high frequency but very low magnitude flows (or low frequency but high magnitude flows) from being assigned as the effective discharge.

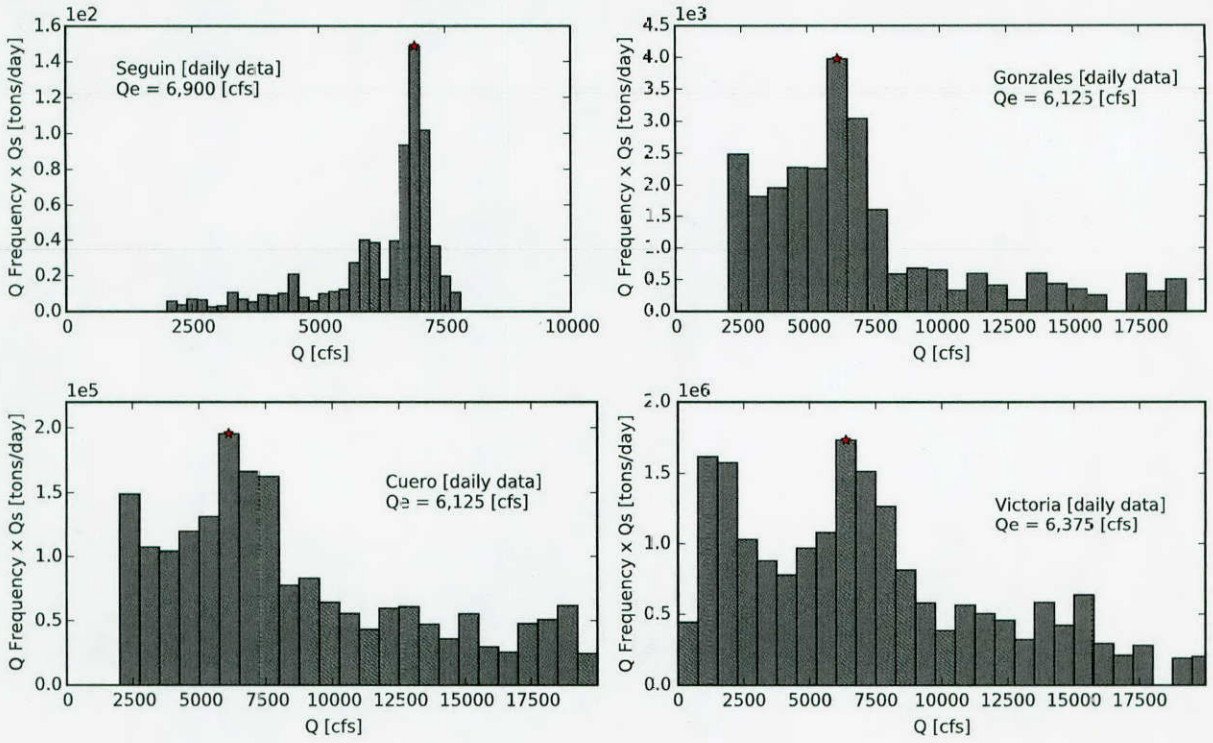

Figure 5.2: Sediment load distributions for Seguin, Gonzales, Cuero, and Victoria using daily flow data.

5.2.4 The effective discharge values

Flows on the Guadalupe can reach extremely large values relative to the typical low flow condition. For example, flows during flood events can reach upwards of 40,000 to 50,000 cfs at Seguin, while 80% of the daily flows are less than 700 cfs (Table 3.1, Figure 4.1). Furthermore, the system is flashy and results in the higher flows only being active for a very short period of time. This is particularly true for the Seguin site. As a result, the daily discharges can be significantly smaller than the 15 min discharge values. For this reason we calculated the effective discharge using both the daily and 15 min flow data. However, in the end, the effective discharge values produced with the 15 min data and the daily flow data were very similar. Considering both types of data, the effective discharge, Q_e, was found to fall between 6,125 and 7,875 cfs at all stations (Table 5.4). In general, Q_e was slightly larger using the 15 min data.

Station	Rating Curve Basis	$Q_{e-daily}$ [cfs]	$Q_{e-15min}$ [cfs]
Seguin	Measured Bed Load	6,900	6,125
Gonzales	Yang (1979) Eq. [Total Load]	6,125	7,625
Cuero	Yang (1979) Eq. [Total Load]	6,125	6,875
Victoria	Yang (1979) Eq. [Total Load]	6,375	7,875

Table 5.4: Calculated effective discharge using the daily, $Q_{e-daily}$, and 15 minute, $Q_{e-15min}$, historic discharge data.

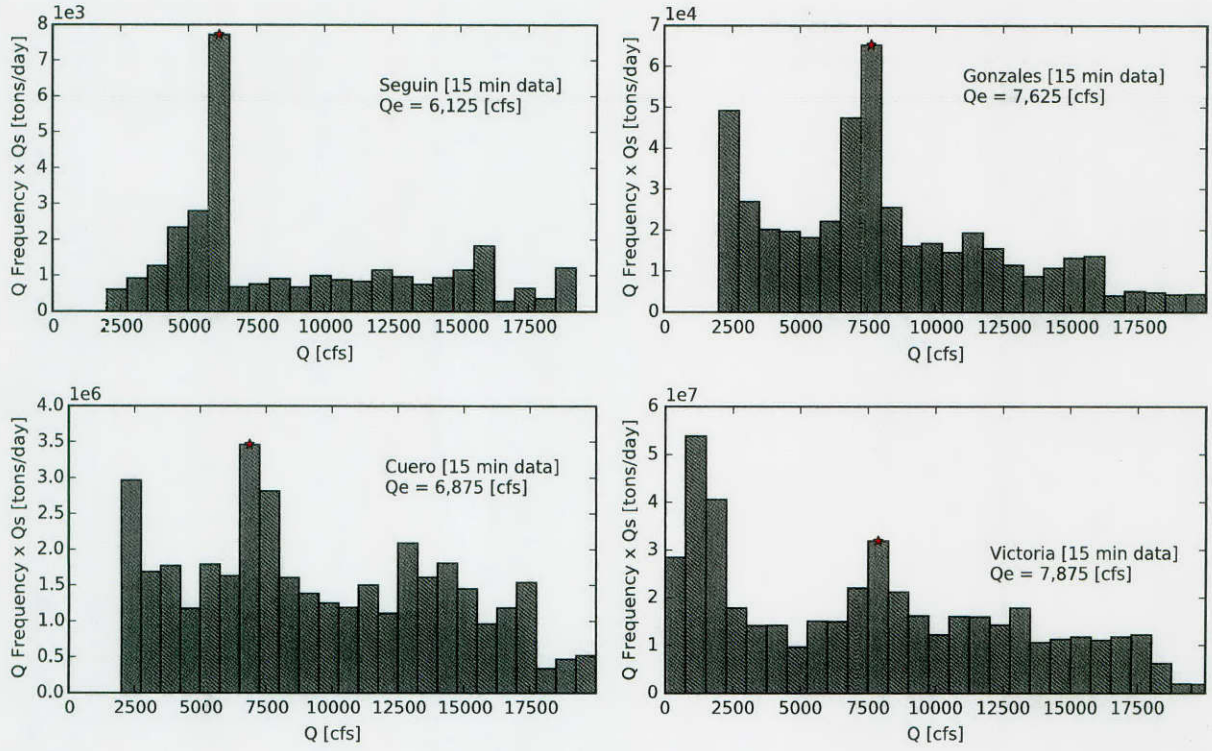

Figure 5.3: Sediment load distributions for Seguin, Gonzales, Cuero, and Victoria using 15 minute flow data.

In addition to the effective discharge, we calculated the half-load sediment discharge, $Q_{1/2}$ from cumulative distributions of the sediment moved as a function of discharge. These values and the cumulative curves for the amount of water and sediment moved during the analysis time period as a function of discharge are shown in figures 5.5 and 5.6. The plots shown in these figures are similar to the suggested summary plots of Klonsky and Vogel (2011). The plots can be used to easily see what the fraction of water moved as flows less than (or greater than) a particular discharge and what percentage of sediment moved this corresponds to. For example, at Seguin (figure 5.5), the figure can be used to see that about 80% of the water volume is moved by discharges less than approximately 750 cfs, but that discharges less than 750 cfs move no bed sediment; in fact, flows of $Q \approx 5{,}500$ cfs and less are only responsible for about 20% of the transported sediment. The plots can also be used to show what the total fraction of sediment moved by flows equal to and less than the effective discharge are. For example, at Victoria, flows equal to and less than the effective discharge ($Q_{e-daily} = 6{,}375$ cfs) are responsible for transporting under 36% of the total sediment load. For visual reference, a flow of $Q \approx 4{,}000$ cfs at the Seguin station is pictured below (figure 5.4).

The half-load discharges varied a bit more from station to station than the Q_e estimates (table 5.5). In general, the half-load estimates are slightly larger than the effective discharge values, and they increase moving from Seguin to Gonzales to Cuero rather than being nearly constant across the three stations (table 5.4 and 5.5). The half-load discharge at Victoria decreases in both the 15 min and daily data because the discharges less than 2,000 cfs are kept in the development of the flow pdf and the sediment transport effectiveness histogram.

Figure 5.4: The Seguin station (A) looking upstream from the downstream side of the road crossing, and (B) looking downstream from the road crossing. The discharge at the time of the photograms is approximately 4,000 cfs.

Station	Rating Curve Basis	$Q_{1/2-daily}$ [cfs]	$Q_{1/2-15min}$ [cfs]
Seguin	Measured Bed Load	6,605	6,095
Gonzales	Yang (1979) Eq. [Total Load]	8,810	10,662
Cuero	Yang (1979) Eq. [Total Load]	10,156	11,288
Victoria	Yang (1979) Eq. [Total Load]	8,961	8,093

Table 5.5: Calculated effective discharge using the daily, $Q_{e-daily}$, and 15 minute, $Q_{e-15min}$, historic discharge data.

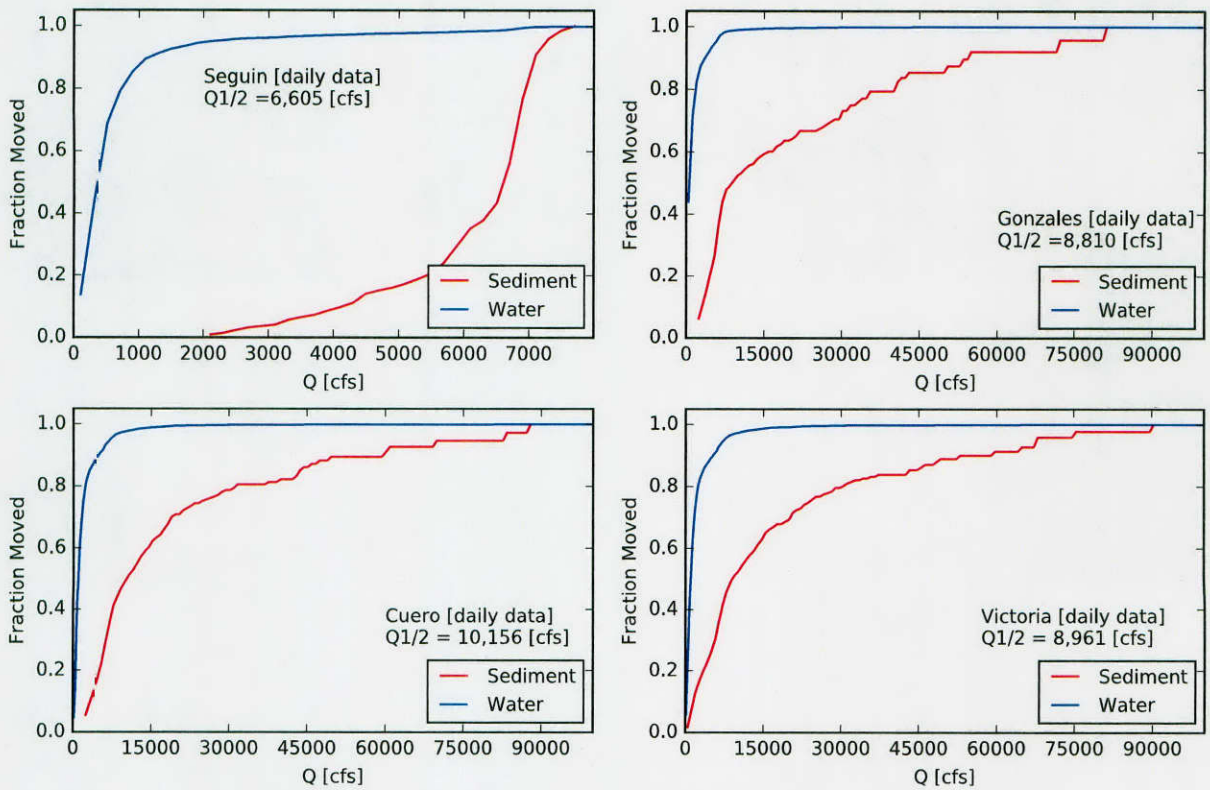

Figure 5.5: Summary plots showing the cumulative fraction of flow and sediment moved as a function of discharge using the daily flow data.

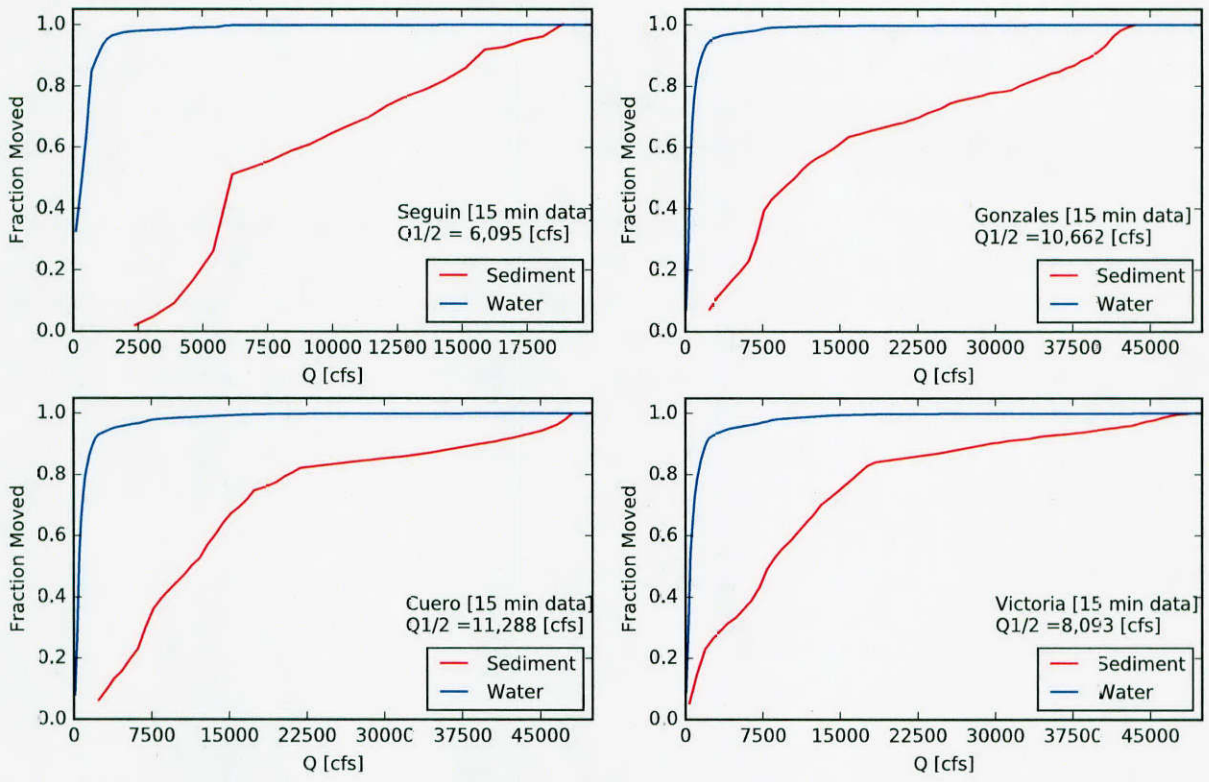

Figure 5.6: Summary plots showing the cumulative fraction of flow and sediment moved as a function of discharge using the 15 min flow data.

5.2.5 *Relation between effective discharge, half-load discharge, and bankfull discharge*

A reasonable question to ask is how the calculated effective and half-load discharges compare with (1) the bankfull discharge, and (2) the 1.5 and 2 year return period flows at each of the sites. A description of how each of these values was calculated has been given above for all discharges other than the bankfull discharge. The bankfull discharge, Q_{bf} is defined as the discharge that just fills the main channel up to the top of its banks with water. There are two primary methods for calculating the bankfull state. In the first, the bankfull cross section can be defined in the field using the geometric properties of the cross section and vegetation indicators. The discharge can then be calculated knowing the bankfull geometry, the channel slope, and the roughness coefficient (such as the Manning n value). It can also be defined using a measured range of discharges and geometric properties, e.g., stage or top width as a function of discharge. In this study, we have calculated the bankfull discharge using USGS field measured stage-discharge data at each site. With this second method, the bankfull state is defined as the discharge after which there is a change in the stage-discharge functionality. The slope break can be viewed as the discharge at which water begins to spill out of the main channel and onto the wider flood plain.

The estimated bankfull discharges are listed in Table 5.6 along with the other dominant discharge estimators. For Q_e and $Q_{1/2}$ we have opted to use the daily flow data. The bankfull discharge increases moving from Seguin to Gonzalez, but then remains approximately constant for the lower three stations. This trend is consistent with the general return period flow statistics, which show little systematic change moving from Gonzalez to Victoria for flows greater than a two year flood (Table 3.1). At all stations, the bankfull discharge is larger than the 2 year return period flow. In general, the effective discharge is smaller than both the half-load and 1.5 year flood (except at Seguin), and the half-load is quite close in magnitude and trend to the 1.5 year flood.

Station	Rating Curve Basis	Sed. + Flow		Flow		
		Q_e [cfs]	$Q_{1/2}$ [cfs]	$Q_{1.5}$ [cfs]	Q_2 [cfs]	Q_{bf} [cfs]
Seguin	Measured Bed Load	6,900	6,605	5,723	8,330	11,000
Gonzales	Yang (1979) Eq. [Total Load]	6,125	8,810	8,408	15,609	20,000
Cuero	Yang (1979) Eq. [Total Load]	6,875	10,156	11,092	15,300	20,000
Victoria	Yang (1979) Eq. [Total Load]	6,375	8,961	11,600	16,500	18,000

Table 5.6: Comparison of the effective discharge, Q_e, the half-load discharges, $Q_{1/2}$, and the pure flow statistics of the 1.5 and 2 year return period flows, $Q_{1.5}$ and Q_2, and the bankfull discharge, Q_{bf}.

6 Conclusions

6.1 Summary

Measurements of channel cross sectional geometry, bed sediment, and suspended sediment concentration were made periodically between January 1, 2014 and April 30, 2015 at four USGS gaging stations along the Guadalupe River; namely the Seguin, Gonzales, Cuero, and Victoria stations. Bed load transport rates were also measured at the most upstream station (Seguin) over low, moderate, and high discharges to provide the data needed to develop a sediment load rating curve based on measured data for the station. For the remaining three stations, reach property measurements were coupled with sediment transport equations to develop sediment load rating curves. The sediment load rating curves were then used in conjunction with daily and 15-min USGS discharge data to calculate the effective discharge at each of the four stations. Sediment half-load discharges and cross sectional bankfull discharges were also calculated.

6.2 Primary findings

Field observations and calculations both suggest that bed load is the primary mode of transport at the Seguin, Gonzales, and Cuero sites, and that little bed sediment is moved at discharges less than 2,000 cfs. For flows above 2,000 cfs, the bed load rating curve for the Seguin station was found to be $Q_b = \alpha Q^{\beta}$ with $\alpha = 1E^{-10}$ and $\beta = 2.3376$. Rating curves for the remaining three sites were developed using an array of standard bed load and total load equations. The β value resulting from these calculations ranged from 1 to 2 with the majority falling between 1.5 and 1.7. Calculated effective discharges were nearly constant across all sites, ranging from 6,200 to 6,900 cfs when using the daily flow data. Variation from station to station increased slightly when using the 15-min data, producing a slight increase in Q_e moving downstream and an overall range of approximately 6,100 to 7,900 cfs. Simple analysis of the yearly peak flow data at the four stations showed that the 1.5 and 2 year floods all increase moving downstream, with the 1.5 year flood increasing from 5,700 cfs to 11,600 cfs from Seguin to Victoria. Half-load discharges were slightly larger than the effective discharges and showed a general increase in value moving downstream from Seguin. Both the effective and half-load discharge were near, but smaller than, the 1.5 year flood at each station. All of the effective, half-load, 1.5 year, and 2 year flows were smaller than the bankfull discharge calculated using the USGS stage-discharge data. This is due to the high banks in this reach of the Guadalupe. A summary of the calculated flows can be found in table 5.6.

6.3 Secondary finding

In the event that the sediment rating curve must be developed using sediment transport equations, in place of measured transport rates, then the selection of the transport equation is far more influential on the Q_e estimates than any data collected at the reach of interest. This is because the β value in the rating curve is fairly insensitive to grain size, channel slope, channel

width, or the exact cross sectional shape used in the analysis. Therefore, if sediment transport rates are not measured, there is little need to collect much onsite data past what is needed to aid in selecting an appropriate transport equation. This secondary conclusion is based on the analytic analysis presented in section 2.3 and the empirical evidence played out in the calculation of Q_e at the three downstream stations (Gonzales, Cuero, and Victoria).

References

Andrews, E. D. (1980). Effective and Bankfull Discharges of Streams in the Yampa River Basin, Colorado and Wyoming. *Journal of Hydrology*, 46(3-4):311–330.

Asquith, W. H. and Slade, R. M. (1997). Regional equations for estimation of peak- streamflow frequency for natural basins in texas. Technical report, U.S. Geological Survey and U.S. Department of the Interior.

ASTM (2007). ASTM D3977 - 97(2007) Standard Test Methods for Determining Sediment Concentration in Water Samples. *American Society for Testing and Materials*, 11.02.

Barry, J. J., Buffington, J. M., and King, J. G. (2004). A general power equation for predicting bed load transport rates in gravel bed rivers. *Water Resources Research*, 40:W10401.

Biedenharn, D. S., Copeland, R. R., Thorne, C. R., Soar, P. J., Hey, R. D., and Watson, C. C. (2000). Effective Discharge Calculation: A Practical Guide. ERDC/CHL TR-00-15, U.S. Army Engineer Research and Development Center, Coastal and Hydraulics Laboratory.

Bunte, K., Abt, S. R., Potyondy, J. P., and Swingle, K. W. (2008). A comparison of coarse bedload transport measured with bedload traps and helley-smith samplers. *Geodinamica Acta*, 21(1-2):53–66.

Crowder, D. W. and Knapp, H. V. (2005). Effective Discharge Recurrence Intervals of Illinois Streams. *Geomorphology*, 64(3-4):167 – 184.

Diplas, P., Kuhnle, R., Gray, J., Glysson, D., and Edwards, T. (2008). *Sedimentation Engineering: Processes, Measurements, Modeling, and Practice - Sediment Transport Measurements*, chapter 5, pages 307–353. ASCE Manuals and Reports on Engineering Practice No. 110. American Society of Civil Engineering.

Emmett, W. and Wolman, M. (2001). Effective Discharge and Gravel-bed Rivers. *Earth Surface Processes and Landforms*, 26(13):1369–1380.

Engelund, F. and Hansen, E. (1967). *A Monograph on Sediment Transport to Alluvial Streams.* Teknik Vorlag, Copenhagen.

Francalanci, S., Paris, E., and Solari, L. (2013). A combined field sampling-modeling approach for computing sediment transport during flash floods in a gravel-bed stream. *Water Resources Research*, 49(10):6642–6655.

Hey, R. D. (1997). Channel Response and Channel Forming Discharge: Literature Review and Interpretation. Final Report U.S. Army Contract Number R&D 6871-EN-01.

Klonsky, L. and Vogel, R. M. (2011). Effective Measures of "Effective" Discharge. *The Journal of Geology*, 119(1):1–14.

Lane, E. W. (1955). The Importance of Fluvial Morphology in Hydraulic Engineering. *Proc., ASCE*, 81(745):1–17.

Lenzi, M., Mao, L., and Comiti, F. (2006). Effective Discharge for Sediment Transport in a Mountain River: Computational Approaches and Geomorphic Effectiveness. *Journal of Hydrology*, 326(1-4):257–276.

Ma, Y., Huang, H. Q., Xu, J., Brierley, G. J., and Yao, Z. (2010). Variability of Effective Discharge for Suspended Sediment Transport in a Large Semi-arid River Basin. *Journal of Hydrology*, 388(3-4):357 – 369.

Mackin, J. H. (1948). Concept of the Graded River. *Geological Society of America*, 59:463–512.

Meyer-Peter, E. and Müller, R. (1948). Formulas for bed-load transport. In *Proceedings of the Second Meeting*, pages 39–64, Stockholm, Sweden. IAHR.

Pickup, G. and Warner, R. (1976). Effects of Hydrologic Regime on Magnitude and Frequency of Dominant Discharge. *Journal of Hydrology*, 29(1-2):51–75.

Sichingabula, H. M. (1999). Magnitude-frequency Characteristics of Effective Discharge for Suspended Sediment Transport, Fraser River, British Columbia, Canada. *Hydrological Processes*, 13(9):1361–1380.

Vogel, R. M., Stedinger, J. R., and Hooper, R. P. (2003). Discharge Indices for Water Quality Loads. *Water Resources Research*, 39(10):1273.

Whiting, P. J., Stamm, J. F., Moog, D. B., and Orndorff, R. L. (1999). Sediment-transporting flows in headwater streams. *Geological Society of America Bulletin*, 111(3):450–466.

Wolman, M. G. and Miller, J. C. (1960). Magnitude and Frequency of Forces in Geomorphic Processes. *Journal of Geology*, 68:54–74.

Wong, M. and Parker, G. (2006). Reanalysis and correction of bed-load relation of meyer-peter and müller using their own database. *Journal of Hydraulic Engineering*, 132(11):1159–1168.

Yang, C. T. (1979). Unit Stream Power Equations for Total Load. *Journal of Hydrology*, 40(1-2):123 – 138.